ISSN1346－7832

独立行政法人港湾空港技術研究所

港湾空港技術研究所報告

REPORT OF THE PORT AND AIRPORT RESEARCH INSTITUTE

VOL.41 NO.1 March 2002

NAGASE, YOKOSUKA, JAPAN

INDEPENDENT ADMINISTRATIVE INSTITUTION,
PORT AND AIRPORT RESEARCH INSTITUTE

港湾空港技術研究所報告（REPORT OF PARI）
第 41 巻　第 1 号（Vol. 41, No. 1），　2002年3月（March 2002）

目　　次（CONTENTS）

REPORT OF THE PORT AND AIRPORT RESEARCH INSTITUTE Vol. 41, No. 1

Factors Affecting Nutrient Cycling in Intertidal Sandflats

Tomohiro KUWAE*

Synopsis

The present study aimed to improve our understanding of nutrient cycling in intertidal sandflats. Special emphasis was placed on the biogeochemical role of benthic microorganisms, including bacteria and microalgae, in nutrient removal from coastal areas. This paper consisted of three main parts: (1) the method used for the counting and sizing of benthic bacteria, as required for the quantification of various bacterial roles in sediments (Chapter 2), (2) the biogeochemical role of intertidal sandflats during immersion (Chapter 3), and (3) the biogeochemical role of intertidal sandflats during emersion and inundation (Chapter 4). In Chapter 2, the author reported a new dual-staining technique using both 4′,6-diamidino-2-phenylindole (DAPI) and acridine orange (AO) for estimating the abundance and biovolume of benthic bacteria. The effect of dispersion procedures and sediment characteristics on bacterial enumeration and sizing was also investigated. In Chapter 3, the author reported the simultaneously measured rates of nitrification, denitrification, sediment-water nutrient exchange, and sedimentary oxygen production in the Banzu intertidal sandflat located in Tokyo Bay. These data were then used to assess the relative importance of different processes on spatial and temporal variation in sediment-water nutrient exchange fluxes and denitrification in the intertidal sandflat. In Chapter 4, tide-induced temporal changes in the concentrations of three porewater nutrient species (nitrate, ammonium, and phosphate) during different seasons were investigated to elucidate the effect of tidal cycles on porewater nutrient dynamics in the Banzu intertidal sandflat. The author focused on (1) the influence of diffusive fluxes and advective transport on nutrient pool sizes during emersion and inundation; and (2) the role of emersion in microbial processes, including nitrification and nitrate reduction.

Key Words: eutrophication, microbial processes, nitrogen and phosphorus cycles, Banzu tidal flat, Tokyo Bay

*Senior Researcher, Marine Environment and Engineering Department, Port and Airport Research Institute
3–1–1, Nagase, Yokosuka 239–0826, Japan
Phone: +81–468–44–5046; Fax: +81–468–44–1274; E-mail: kuwae@ipc.pari.go.jp

港湾空港技術研究所報告
第41巻第1号（2002.3）

砂質干潟の栄養塩循環に影響をおよぼす要因

桑江 朝比呂*

要　旨

干潟に生息するバクテリアや微細藻類などの微生物による栄養塩除去機能を解明するため，砂質干潟における栄養塩循環を定量化し，その特性やメカニズムについて検討した．はじめに，底生バクテリアの機能の定量化に必要とされる細胞数と細胞体積の測定に関する方法を検討し，以下の結論を得た．(1) 本研究で開発された二重染色法により，従来法よりも明瞭かつ客観的にバクテリアと他物質とを区別して測定することが可能となった．(2) バクテリアを底泥粒子から分散させるため，ホモジェナイザー・超音波洗浄器・超音波破砕器の3つの機器をを用いて処理効率を比較した結果，超音波破砕器がもっともすぐれていることがわかった．(3) 小さなバクテリアほど分散に時間を要するため，細胞体積のサイズ分布を把握するためには，分散処理時間を長くした方がよいことがわかった．次に，砂質干潟の冠水時における栄養塩循環について検討し，以下の結論を得た．(1) 夏季の暗条件におけるアンモニア態窒素を除き，すべての栄養塩は季節や光条件にかかわらず干潟底泥によって除去された．(2) 栄養塩の除去量は光条件に大きく左右された．これは底泥表面に存在する微細藻類が明条件下で活発に栄養塩を取り込んだためと考えられた．(3) アンモニア態窒素フラックスにおいてみられた季節性やサンプル間のばらつきといった時空間的変動には，アサリによるアンモニア態窒素の排泄が大きく寄与していた．(4) 底生微細藻類により取り込まれた溶存無機窒素のうち，31%は直上水由来であった．(5) 底泥間隙水中の硝酸態窒素が脱窒の主要な供給源であり，直上水由来の硝酸態窒素の寄与は小さかった．最後に，砂質干潟の干出時および冠水直後における栄養塩循環について検討し，以下の結論を得た．(1) 干出時間が短く，地形勾配の緩い干潟では，干潟底泥が干出した後も含水率の低下がみられなかった．したがって，間隙水位の変動によってもたらされる間隙水栄養塩の移流は無視できることがわかった．(2) 底泥表層における硝酸態窒素およびリン酸態リン濃度の急な勾配により，大きな下向きの拡散フラックスが発生し，底泥表層における栄養塩濃度の変化に大きく寄与していた．(3) 底泥亜表層における脱窒や異化的アンモニア生成といった硝酸還元反応は，分子拡散によって底泥表層から供給される硝酸態窒素によって支えられていた．(4) 干出後の時間経過に伴い，底泥亜表層における酸化還元環境が酸化的に変化した．これにより，硝酸態窒素の生成が促進され，アンモニア態窒素の生成が抑制された．(5) 冠水直後に，外力による乱流混合やバイオターベーションなどにより，底泥中の栄養塩量が激減した．以上のように，本研究によって，砂質干潟における栄養塩のストックおよびフローが冠水時および干出時の両相において初めて定量化され，その特性や主要なメカニズムが明らかとなった．

キーワード：富栄養化，微生物過程，窒素・リン循環，盤洲干潟，東京湾

* 海洋・水工部 主任研究官
〒239-0826 横須賀市長瀬3-1-1 独立行政法人 港湾空港技術研究所
Phone: +81-468-44-5046, Fax:+81-468-44-1274, E-mail: kuwae@ipc.pari.go.jp

CONTENTS

1. Introduction

Broad intertidal sand and mudflats fringe the coastlines of many countries in mid-latitude, meso- and macro-tidal environments (Mathieson and Nienhuis, 1991). These areas form extensive low-slope flats, being regularly exposed and submerged by tides. Despite the extreme rhythmic variations in temperature and salinity, these coastal deposits form one of the most productive natural ecosystems on Earth, with a gross primary productivity equal to many more familiar terrestrial systems (Odum, 1971). Intertidal flats support a rich benthic community and provide an indispensable feeding ground for many species of shorebirds (**Figure 1**). They form an integral and important part of coastal ecosystems, which have been usefully exploited by humans for port facilities, waste disposal, and amenity development for centuries (Eco-port Technical Working Group, 1998).

Attempts to take advantage of these diverse functions can lead to conflicts in planning and management (e.g. the recent typical conflicts of the Fujimae intertidal flat and the Isahaya intertidal flat in Japan). Conflict arises because the various way in which intertidal flats can be exploited are not all necessarily compatible. The need for resolution of these conflicts is placing heavy demands on coastal managers and is becoming increasingly urgent as human population pressure increases and as the public shows a greater appreciation for the natural value of coastal areas. The "Eco-port Policy" proposed by the former Ministry of Transport, Japan, reformed the Ministry of Land, Infrastructure and Transport, Japan, in January 2001, is currently enhancing the accumulation of knowledge and technology focused on the harmonization of coastal development and adjacent natural ecosystems (Ports and Harbours Bureau, Ministry of Transport, Japan, 1997). In practice, habitat loss in coastal and estuarine areas is increasingly mitigated by the restoration of existing habitats or by the creation of new habitats (Hosokawa, 2000). For such habitat restoration to be successful requires a thorough understanding of biological and sedimentological interactions as well as changing atmospheric and oceanographic forces, on a variety of spatial and temporal scales. It is only through increased understanding of intertidal flat dynamics founded on a solid base of knowledge that we will be able to manage these coastal environments both effectively and efficiently.

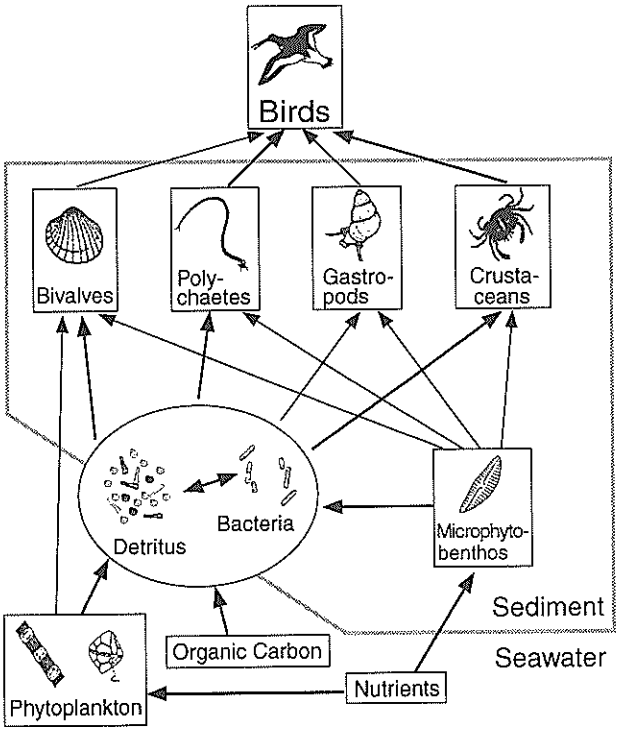

Figure 1 Representative food web for intertidal flat ecosystems

Of the biological and sedimentological interactions that influence intertidal flat dynamics, some of the most important processes are nutrient cycling. Eutrophication — an increased rate of supply of nutrients leading to enhanced primary production — is caused mainly by nutrient loading (and secondarily by organic matter) derived from terrestrial sources. Thus, many coastal environments, located at the interfaces between land and the open sea, have suffered from accelerated eutrophication. In this situation, the cycling of nitrogen and phosphorus is particularly important, as it is often the major limiting element for algal productivity in coastal areas.

The major transformation processes of the nitrogen cycle in intertidal flats are mineralization, nitrification, denitrification, dissimilatory nitrate reduction, assimilation, and excretion by macrofauna (**Figure 2**). Denitrification is a crucial process, being the major pathway by which nitrogen is lost within ecosystems. On the other hand, intertidal sediments often have characteristically high levels of benthic microalgal biomass and productivity (e.g. Colijn and de Jonge, 1984; Varela and Penas, 1985; Cammen, 1991). Photosynthetic processes can result in large diurnal change in nutrient demands and affect the nutrient cycle near the sediment surface.

Although the importance of intertidal sediments in nutrient cycling within Japanese coastal areas has been discussed (Kurihara, 1988; Sasaki, 1989), the quantification of nutrient pathways is established in only a few studies (Nakata and Hata, 1990; Aoyama et al., 1996; Montani et al., 1998; Kodama et al., 2000; Magni et al., 2000; Sayama, 2000). Further, while the biogeochemistry of eutrophic intertidal sediments during immersion has been studied elsewhere in relation to the sediment-water column exchange of nutrients (e.g. Falcão and Vale, 1990; Middelburg et al., 1995; Asmus et al., 1998;

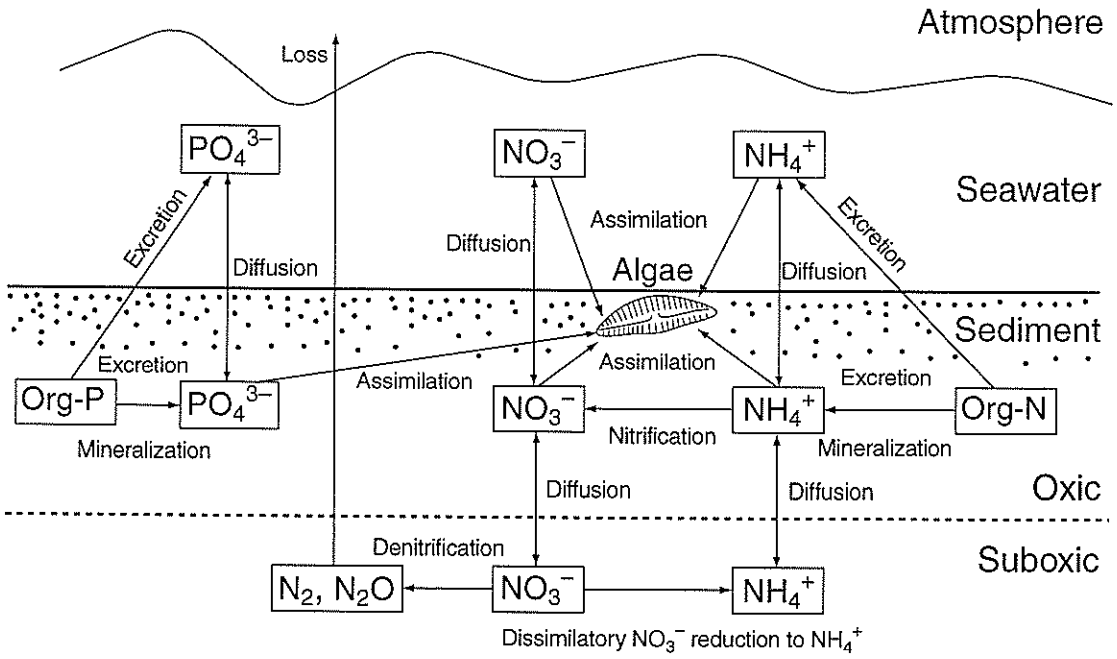

Figure 2 Biogeochemistry of intertidal flats showing the major processes considered during the present study

Kuwae et al., 1998; Mortimer et al., 1999; Cabrita and Brotas, 2000), little is yet known of the dynamics of nutrients in such sediments during emersion or transitional periods (Kerner et al., 1990; Rocha, 1998; Rocha and Cabral, 1998; Usui et al., 1998).

Another poorly understood aspect of nutrient cycling in intertidal sediments is the role played by sediment bacteria. Bacteria are not the only organisms involved in mineralization processes, but they play a central role in the transformation of matter and energy in natural ecosystems. However, these roles of sediment bacteria have not been fully reconciled as they have for pelagic bacteria (Alongi, 1998). The reason for the relatively poor understanding of sediment bacteria is that it is much more difficult to sample and isolate organisms and organic matter from inorganic sediment particles. Sampling and isolating difficulties arise because sediment bacteria intertwine with and stick to organic coatings, including their own mucus. Recent improvements in the techniques have somewhat circumvented these problems (e.g. Bloem et al., 1995; Epstein and Rossel, 1995; Blackburn et al., 1998; Kuwae and Hosokawa, 1999), but sedimentary biota are still more difficult to study than pelagic organisms.

The present study aims to improve our understanding of nutrient cycling in intertidal sandflats. I will focus on the biogeochemical role of benthic microorganisms, including bacteria and microalgae, in nutrient removal from coastal areas. This study consists of three main parts: (1) the method used for the counting and sizing of benthic bacteria, as required for the quantification of various bacterial roles in sediments (**Chapter 2**), (2) the biogeochemical role of intertidal sandflats during immersion (**Chapter 3**), and (3) the biogeochemical role of intertidal sandflats during emersion and inundation (**Chapter 4**). In **Chapter 2**, I report a new dual-staining technique using both 4′,6-diamidino-2-phenylindole (DAPI) and acridine orange (AO) for estimating the abundance and biovolume of benthic bacteria. I also investigate the effect of dispersion procedures and sediment characteristics on bacterial enumeration and sizing. In **Chapter 3**, I report the simultaneously measured rates of nitrification, denitrification, sediment-water nutrient exchange, and sedimentary oxygen production in the Banzu intertidal sandflat located in Tokyo Bay. These data are then used to assess the relative importance of different processes on spatial and temporal variation in sediment-water nutrient exchange fluxes and denitrification in the intertidal sandflat. In **Chapter 4**, I report the effect of tidal cycles on porewater nutrient dynamics in the Banzu intertidal sandflat. To my knowledge, this is the first report dealing with tide-induced temporal changes in the concentrations of three porewater nutrient species (nitrate, ammonium, and phosphate) during different seasons. Special emphasis is placed on (1) the influence of diffusive fluxes and advective transport on nutrient pool sizes during emersion and inundation; and (2) the role of emersion in microbial processes, including nitrification and nitrate reduction.

2. Determination of Abundance and Biovolume of Bacteria in Sediments

2.1 Introduction

The importance of bacteria in marine and estuarine sediments as a food source and major contributor to biogeochemical processes in benthic ecosystems has been widely recognized (e.g. Montagna, 1984; Alongi, 1988; Cowan et al., 1996; Kuwae et al., 1998). The quantification of bacterial roles requires precise measurement of their abundance and biovolume. A standard procedure used to determine bacterial cell abundance and biovolume is the microscopic examination of fluorescently stained cells with either 4′,6-diamidino-2-phenylindole (DAPI) or acridine orange (AO). Most benthic bacteria are attached to sediment particles with extracellular polymeric substances (EPS), in contrast to free-living bacteria in water columns. Thus, a direct measurement of the abundance and biovolume of benthic bacteria by epifluorescence microscopy is possible only when bacteria can be detached or segregated from aggregates that include mineral particles and detritus.

Factors affecting the accuracy of microscopic examination have been reported for the sample dilution and staining procedure (Schallenberg et al., 1989) and for the efficiency of bacterial cell dispersion, including the type of equipment, treatment time, and intensity of dispersion (Epstein and Rossel, 1995). DAPI specifically binds with nucleic acids and emits a brilliant blue light under UV excitation, enabling bacteria to be segregated more easily than with AO, which also dyes other intracellular structures in addition to nucleic acids. In the case of poor sample dilution, however, the problems of background fluorescence still remain even with DAPI staining. Several instruments are available to disperse bacterial cells from aggregates. Ultrasonic cleaners and ultrasonicators (Venji and Albright, 1986; Schallenberg et al., 1989; Epstein and Rossel, 1995) disperse bacteria by the vibration of individual particles, while tissue homogenizers (Dye, 1983; Imai, 1987; Alongi, 1988) mechanically break sediments into smaller particles. The time and intensity of sediment dispersion strongly affect bacterial cell counts (Epstein and Rossel, 1995) and size distribution. More intense treatments over longer timescales tend to decrease the aggregate masking effect, leading to an increase in the bacterial cell counts. However, with the longer and more intense dispersion, the tendency for cell destruction is higher. Moreover, the efficiency of bacterial cell dispersion is affected by sediment characteristics, such as viscosity and grain size distribution (Dye, 1983).

In this chapter, I report a new dual-staining technique using both DAPI and AO for estimating the abundance and biovolume of benthic bacteria. I also explain the effect of sediment characteristics and dispersion procedures on the abundance and size of separated bacterial cells. The present study investigates the intertidal sediments from Tokyo Bay, Japan.

2.2 Materials and Methods

2.2.1 Sampling

Samples were obtained in May 1998 from three sites on the coast of Tokyo Bay, Japan: a sandy beach (35°10.6′N, 139°39.5′E), an intertidal sandflat (35°24.2′N, 139°54.2′E), and a mudflat (35°8.5′N, 139°39.9′E) (**Figure 3**). Core samples were taken to a depth of 5 cm with acrylic core tubes (8.6-cm internal diameter). Each sample was thoroughly mixed and immediately brought back to the laboratory. Dispersion procedures were applied to sediments obtained by subsampling. Subsamples (0.3 g) were mixed with 5 ml of filter-sterilized seawater (particle-free water) in acid-washed polycarbonate tubes (10 ml) and stored at 4°C. The particle-free water was obtained by two filtrations of 10% formalin-seawater solution buffered with sodium tetraborate (final concentration, 35.1 g liter^{-1}) (Alongi, 1988) using Millipore filters (0.22-μm pore size).

2.2.2 Procedures for dispersion and bacterial cell counting

Prior to dispersion, the samples were incubated for at least 15 min with the surfactant Tween 80 (final concentration, 1 mg liter^{-1}). Tween 80 facilitates an even distribution of bacteria on the membrane filter (Epstein and Rossel, 1995). Three different devices were used to disperse bacteria from the sediments: an ultrasonic cleaner (B-2200; Branson) (60-W output), an ultrasonicator (GE-100; Biomic) (100-W output) equipped with a 3-mm tapered microtip and with the amplitude set at 40% of the maximum, and a homogenizer (PT-2000; Kinematica) set at 20,000 rpm. The dispersion time for samples in the tubes was 5 to 60 min for the ultrasonic cleaner and 0.5 to 8 min for the others. To prevent possible denaturation of nucleic acids caused by overheating, the tubes were placed in ice water during the dispersion treatments (Epstein and Rossel, 1995).

After dispersion, the samples were diluted 50 to 250 times (final dilution, 830 to 4,160) with particle-free seawater. Diluted samples were dual stained with a combination of DAPI to a final concentration of 5 μg ml^{-1} (Schallenberg et al., 1989) and AO to a final concentration of 1 mg ml^{-1} for counterstaining. After more than 30 min of staining, 0.5 to 2 ml of each sample was filtered through a polycarbonate black filter (0.2-μm pore size) and then rinsed with particle-free seawater. The filters were immersed in nonfluorescent oil on microscope slides and covered with coverslips. Within 24 h of the dispersion procedure, bacteria retained on the filters were examined under an Olympus BX-FLA-3

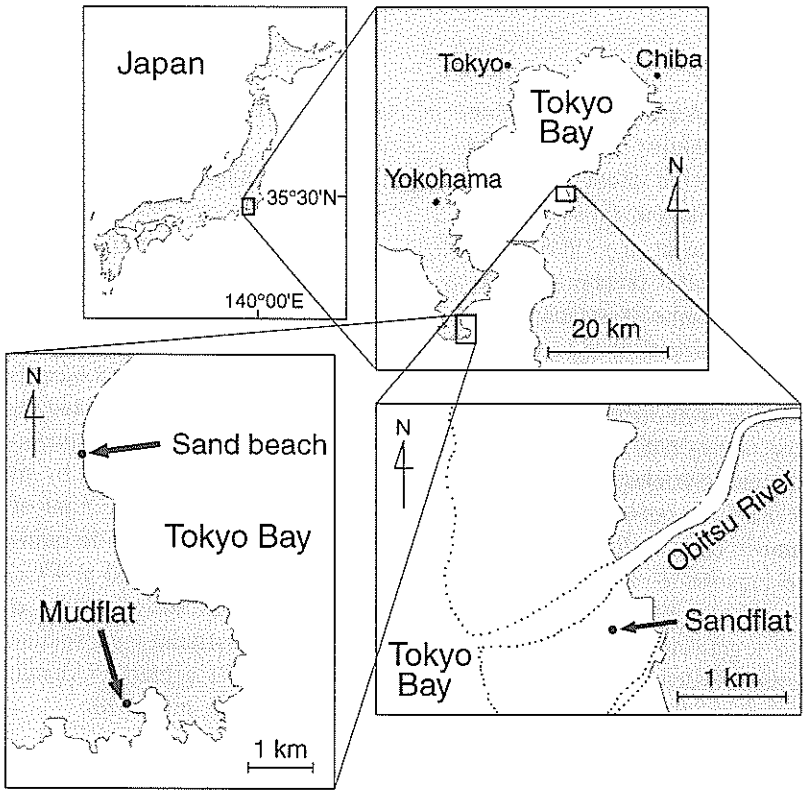

Figure 3 Location of the sampling site in Tokyo Bay. Dotted line indicates the lowest tidal level.

epifluorescence microscope (UV excitation) equipped with a 100× oil immersion objective. On each filter, no fewer than 200 clear-edged cells in 20 microscopic fields were counted.

2.2.3 Measurement of bacterial cell volume

After dispersion, the samples were centrifuged (100 × g) for 5 min in order to exclude nonbacterial particles as much as possible. Supernatants were dual stained and filtered as described above. A camera (TM-10AK; Olympus) mounted on the microscope was used to take microphotographs on color slide films. Images on the films were scanned with a film scanner (QuickScan 35; Minolta) connected to a computer and digitized, and thresholds were determined using image analysis software (Image 1.59; NIH). Thresholds were manually adjusted by comparing original color images with the digitized image. Bacterial cell-shaped objects were subsequently segregated from other objects, such as detritus and artifacts. Objects with an area less than 6 pixels were automatically excluded from biovolume calculations as noise. Dividing cells, which have two well-defined local intensity maxima, were also removed. The pixel size for the resulting image was 0.17 by 0.17 μm. The project area of an object (A), cell length, and cell width (w) were automatically measured by the image analysis software. To compute the cell volume (V), I considered the rod-shaped cells to be cylinders with a hemispherical cap based on the microscopic observations:

$$V = \pi wA/4 + \pi w^3/6 - \pi^2 w^3/16 \qquad (1)$$

At least 500 bacterial cell-shaped images were analyzed per sample.

2.2.4 Sediment characteristics

At each study site, water content, sediment granulometry, and EPS were measured for triplicate samples. The water content was determined by the weight loss when wet sediments were dried at 90°C for 24 h. The grain size was measured by sieving the sediment, and the silt and clay components were determined with a Coulter Multisizer. EPS was examined with the phenol-sulfuric acid assay described by Underwood et al. (1995) as a parameter of viscosity between the bacterial cells and other objects. The amount of EPS is expressed as micrograms of C per gram (dry weight) of sediment, using glucose as a standard.

Table 1 Characteristics of sand beach, sandflat, and mudflat sediments

Site	Wet density ($g\ cm^{-3}$) (mean ± SE)	Dry density ($g\ cm^{-3}$) (mean ± SE)	Water content (%) (mean ± SE)	Porosity (%) (mean ± SE)	Grain size distribution				EPS[a] ($\mu g\ g^{-1}$ dry wt) (mean ± SE)
					Median (μm)	Mud (%)	Silt (%)	Sand (%)	
Sand beach	1.75 ± 0.04	1.39 ± 0.03	20.7 ± 0.2	47.7 ± 1.1	170	0.0	0.4	99.6	17.6 ± 2.1
Sandflat	1.85 ± 0.01	1.38 ± 0.02	25.3 ± 0.4	48.1 ± 0.7	170	0.1	2.4	97.5	49.1 ± 0.8
Mudflat	1.55 ± 0.01	0.85 ± 0.01	45.3 ± 0.4	68.2 ± 0.3	92	4.6	41.2	54.2	354.3 ± 87.2

[a]Measured using glucose as a standard.

2.2.5 Statistical analysis

Statistical differences in bacterial cell counts and sizes among the dispersion time applied to each sediment sample were tested using a one-way analysis of variance (ANOVA). Each ANOVA was followed by a Student-Newman-Keuls (SNK) multiple-comparison test of means. Data sets were tested for homogeneity of variances (Levene test), and the log-transformed values were used if needed for a normal distribution.

2.3 Results

2.3.1 Sediment characteristics

The characteristics of sand beach, sandflat, and mudflat sediments are summarized in **Table 1**. A consistent relationship between sediment granulometry and other sediment characteristics was found. The mudflat sediment exhibited high water and silt contents, with a median grain size of 92 μm. The median grain size in the sandflat was almost the same as that in the sand beach (170 μm); however, the proportion of silt was six times higher in the former. The concentration of EPS was higher in the fine sediment.

2.3.2 Bacterial cell counts

Figure 4 shows the number of dispersed bacteria versus dispersion time for the ultrasonic cleaner, sonicator, and homogenizer techniques for sediments from each site. With both the ultrasonic cleaner and sonicator treatments, the bacterial numbers in samples from all of the sites initially increased with treatment time and then leveled off, resulting in the highest number of bacteria at 15 to 45 min with the ultrasonic cleaner and at 3 to 8 min with the sonicator. However, for the homogenizer treatments, the patterns obtained were totally different from those for the ultrasonic cleaner and sonicator treatments. The highest bacterial numbers were observed in samples subjected to the shortest (0.5- to 2-min) treatment times. The bacterial cell counts then declined steeply as the homogenization time increased, especially

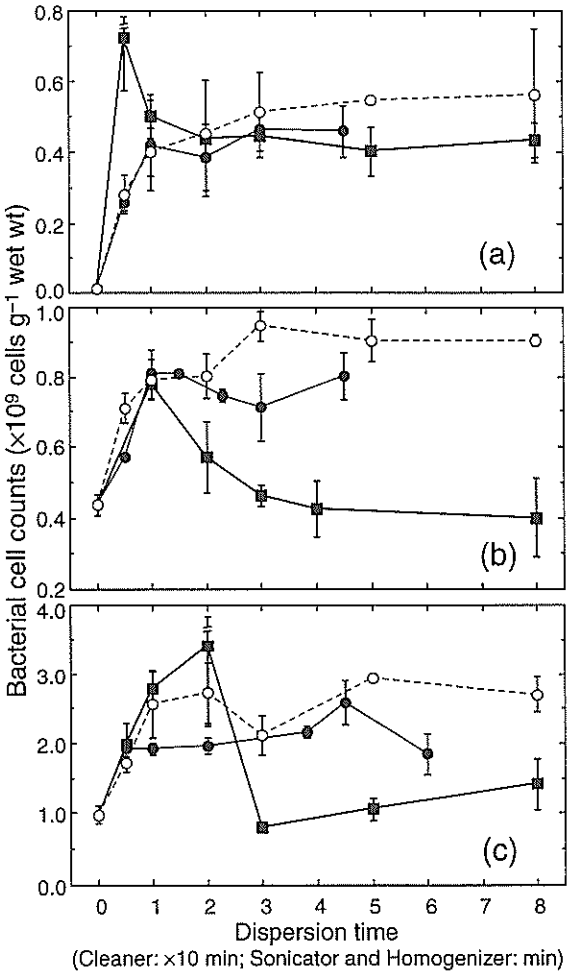

Figure 4 Comparison of the number of dispersed bacteria ($\times 10^9$ cells g^{-1} wet wt) observed after treatment using different dispersal procedures; ultrasonic cleaner (●), sonicator (○), and homogenizer (■) for sediment samples from sandy beach (a), sandflat (b), and mudflat (c). Bars indicate standard errors (n = 3).

Table 2 Maximum number of dispersed bacteria at three sites

Site	Number of cells ($\times 10^9$ g^{-1} wet wt) (mean ± SE) with the following treatment[a]:				Significance at 5% level[b]
	None	Cleaner	Sonicator	Homogenizer	
Sand beach	0.01 ± 0.00	0.40 ± 0.04 (5–45)	0.46 ± 0.04 (0.5–8)	0.49 ± 0.04 (0.5–8)	NS
Sandflat	0.44 ± 0.03	0.78 ± 0.03 (10–45)	0.87 ± 0.03 (1–8)	0.78 ± 0.04 (1)	C H S
Mudflat	0.98 ± 0.12	2.07 ± 0.09 (5–60)	2.61 ± 0.15 (1–8)	2.72 ± 0.41 (0.5–2)	C < S H

[a]The maximum number was calculated by taking the average for a homogenous subset including the maximum mean measured over the dispersion time. Values in parentheses indicate the treatment time (min) for the homogenous subset.

[b]NS, not significant. C, S, and H, ultrasonic cleaner, sonicator, and homogenizer treatment, respectively. Underlining indicates a statistically homogenous group.

in the sandflat and mudflat sediments, where the counts were lower than those observed for nondispersed sediments.

I used the SNK test to examine a statistically homogenous subset including the maximum mean cell count measured over the dispersion time. **Table 2** summarizes the average bacterial cell count in each homogenous subset for each sediment sample and each type of dispersal treatment. The average value was considered to be the maximum value in each case. For both the ultrasonic cleaner and sonicator treatments, the SNK test revealed that the bacterial cell counts were homogenous ($P > 0.05$) over all dispersion times except for several of the shorter dispersion times. For the sand beach sediment, no statistical differences in the maximum numbers were found between samples treated using the three different dispersion techniques. In the sandflat sediment, the maximum number of bacteria found using the ultrasonic cleaner treatment was significantly lower than that found using the sonicator treatment ($0.01 < P < 0.05$). In the mudflat sediment, the maximum number of bacteria found using the ultrasonic cleaner treatment was significantly lower than that found using the sonicator and homogenizer treatments ($0.01 < P < 0.05$).

The more dispersed bacteria were observed in the finer sediments. The maximum number of bacteria found using the sonicator treatment ranged from 0.20×10^9 to 0.94×10^9 cells g^{-1} in the sand beach, from 0.69×10^9 to 1.02×10^9 cells g^{-1} in the sandflat, and from 1.67×10^9 to 3.54×10^9 cells g^{-1} in the mudflat on a wet-sediment basis (**Table 2**). This corresponds to 0.25×10^9 to 1.18×10^9 cells g^{-1}, 0.93×10^9 to 1.37×10^9 cells g^{-1}, and 3.05×10^9 to 6.46×10^9 cells g^{-1} on a dry-sediment basis, respectively. The bacterial numbers in the sandflat and mudflat sediments were approximately two- and fivefold higher, respectively, than those in the sand beach sediment. This tendency was more dis-

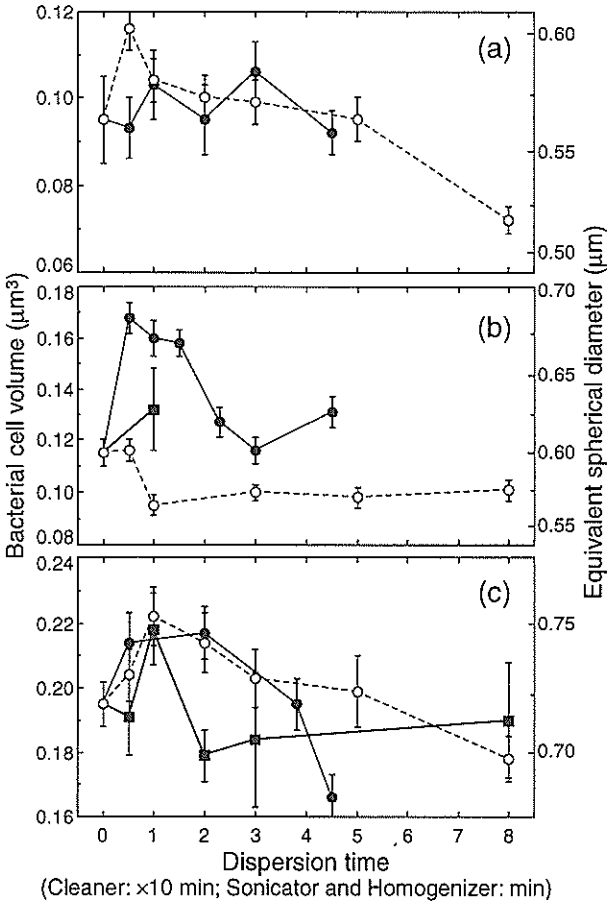

Figure 5 Comparison of dispersed bacterial cell volumes (μm^3) observed after treatment using different dispersal procedures; ultrasonic cleaner (●), sonicator (○), and homogenizer (■) for sediment samples from sandy beach (a), sandflat (b), and mudflat (c). Bars indicate standard errors.

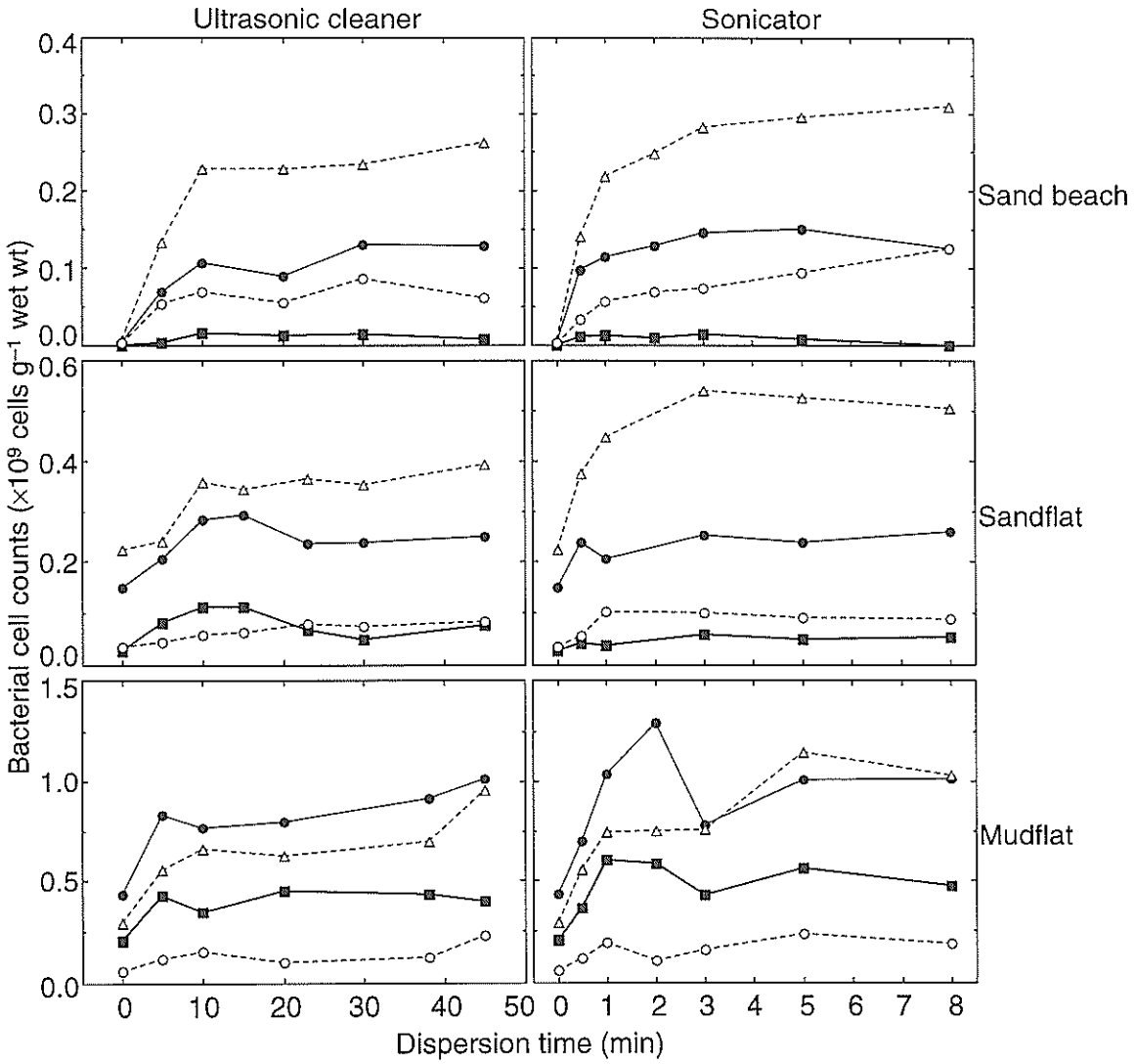

Figure 6 Comparison of the number of size-fractionated bacteria ($\times 10^9$ cells g^{-1} wet wt) by treating samples from the three sites with ultrasonic cleaner and sonicator. Size fraction: <0.03 μm^3 (○); 0.03–0.1 μm^3 (△); 0.1–0.3 μm^3 (●); and >0.3 μm^3 (■).

tinct in the nondispersed samples, for which the counts in the sandflat and mudflat sediments were more than 1 order of magnitude higher than those in the sand beach sediment.

2.3.3 Bacterial cell volume

Figure 5 shows the mean bacterial volume of dispersed bacteria versus dispersion time for sediment samples from each site. For all of the treatments, the biovolumes peaked after a short time interval. The biovolumes then dropped as the dispersion time increased.

To investigate these fluctuation patterns more thoroughly, I divided the bacterial cells counted for the ultrasonic cleaner and sonicator treatments into separate size fractions. The histogram for each data set showed a Guassian-shaped profile (not shown). When the bacterial cells counted were fractionated into four size classes (**Figure 6**), the bacterial cells in the smaller size fractions (<0.1 μm^3) required a longer dispersion time to reach a constant cell count than the larger size fractions (>0.1 μm^3) in each data set. No apparent decline in the cell count was found for either the ultrasonic cleaner or sonicator treatment. These results indicate that the decrease in the mean cell volume over longer dispersion times (**Figure 5**) was caused not by cell destruction but by the increased proportion of smaller cells dispersed from the sediment. Consequently, it was concluded that cell counts over longer treatment times reflect the real size spectrum and are preferable for the accurate estimation of mean bacterial biovolumes. For the homogenizer

Table 3 Biovolume, equivalent spherical diameter, and cell length/width ratio of dispersed bacteria at three sites

Site	Treatment	Time[a] (min)	Biovolume[b] (μm^3) (mean ± SE)	Significance at 5% level[c]	Diameter[b] (μm)	Length/width[b]
Sand beach	None	0	0.095 ± 0.010	S < N C	0.52	1.6
	Cleaner	0–45	0.098 ± 0.003		0.52	1.9
	Sonicator	8	0.072 ± 0.003		0.49	1.8
Sandflat	None	0	0.115 ± 0.005	S < N H C	0.55	1.7
	Cleaner	23–45	0.125 ± 0.003		0.56	1.9
	Sonicator	1–8	0.098 ± 0.002		0.53	1.8
	Homogenizer	0–1	0.117 ± 0.005		0.56	1.7
Mudflat	None	0	0.195 ± 0.007	C S N H	0.66	1.9
	Cleaner	45	0.166 ± 0.007		0.62	2.1
	Sonicator	3–8	0.193 ± 0.005		0.64	2.1
	Homogenizer	1	0.218 ± 0.011		0.66	2.1

[a]Treatment time for a homogenous subset.

[b]Calculated by taking the average for the homogenous subset.

[c]N, C, S, and H, no treatment, ultrasonic cleaner, sonicator, and homogenizer treatment, respectively. Underlining indicates a statistically homogenous group.

treatment, in which only the mudflat sediment was fractionated, all of the bacterial cell fractions dropped steeply after 2 min of treatment (not shown). The size fraction of 0.03 to 0.1 μm^3 dominated in both the sand beach and sandflat sediments, while the size fraction of 0.1 to 0.3 μm^3 dominated in the mudflat. In the sandflat sediment, the cell counts in the 0.03- to 0.1-μm^3 fraction were lower with the ultrasonic cleaner treatment than with the sonicator treatment, which caused the statistical difference in the mean volume between them. In the other sediments, the cell counts for the entire size fraction exhibited nearly similar values.

The mean bacterial biovolume, equivalent spherical diameter, and cell length/width ratio for the three sediment types and dispersion treatments are summarized in **Table 3**. The largest bacterial biovolumes were observed in the finest sediments. Biovolumes ranged from 0.07 to 0.10 μm^3 (0.49- to 0.52-μm equivalent spherical diameter) in the sand beach sediments, from 0.10 to 0.13 μm^3 (0.53 to 0.56 μm) in the sandflat sediments, and from 0.17 to 0.22 μm^3 (0.62 to 0.66 μm) in the mudflat sediments. Similar ranges were also found in the nondispersed samples from the same sites. The cell length/width ratios, which ranged from 1.6 to 2.1, did not significantly differ according to dispersion technique or sediment type ($P > 0.05$).

2.4 Discussion

2.4.1 Dual staining with DAPI and AO

The dual-staining technique utilized in this study can contribute to a better understanding of the bacterial abundance and size distribution in sediments. Until now, either AO or DAPI alone has been used as a dye for benthic bacteria by other workers. If only AO is used for bacterial staining, all of the aggregate components are stained in similar colors, resulting in too low contrast between the bacteria and nonbacterial substances to distinguish between them (**Figure 7a**). Compared with AO staining, DAPI staining provides higher image contrast and is more specific for bacterial staining (Imai, 1987) (**Figure 7b**). However, the problems of background fluorescence also occur when staining with DAPI. In clay- and silt-rich sediments, which are rich in detritus and EPS, the background fluorescence by aggregates containing detritus and minerals as well as bacteria is more intense. When AO and DAPI are used together, under UV light only the bacteria are vividly seen as blue, and the nonbacterial substances are orange (**Figure 7c**). For a counterstaining dye, Epstein and Rossel (1995) proposed the use of Evans Blue. However, based on my observations, AO is superior to Evans Blue in providing contrast to bacteria illuminated blue by DAPI. When the sample is not diluted enough and aggregates accumulate on the filter at a depth greater

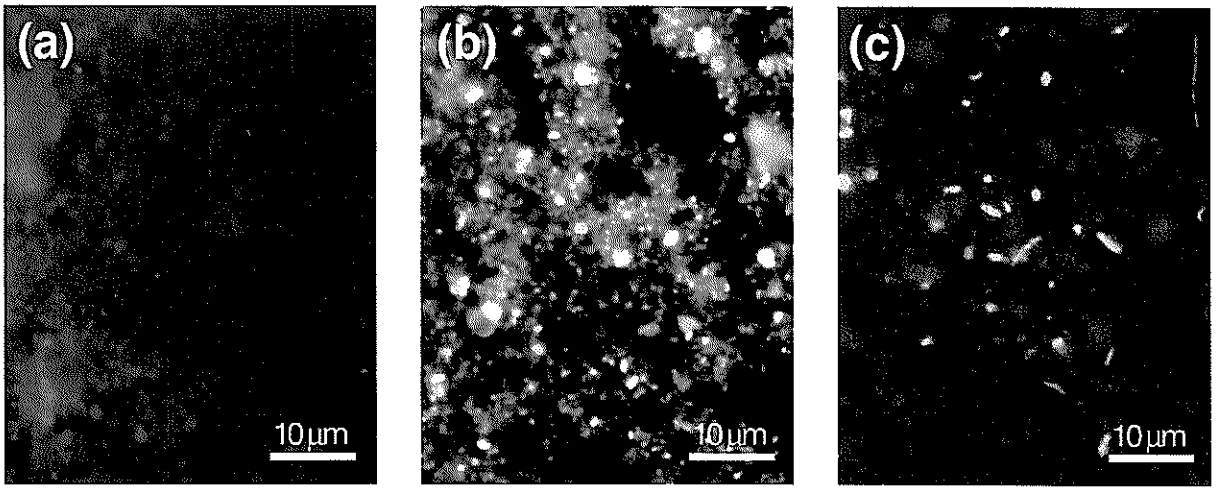

Figure 7 Microphotographs of bacteria stained with AO (a), DAPI (b), and AO + DAPI (c). Scale bars: 10 µm.

than that for proper focus, only part of the cells is in constant focus. This means that nonbacterial substances and background interference will mask the presence of some bacteria, leading to an underestimation of cell abundance (Schallenberg et al., 1989). If this occurs, dual staining can reduce the masking effect, as image contrast is improved and the interference of the background is reduced. Consequently, dual staining simultaneously overcomes the problems of low contrast in the AO technique and background interference in the DAPI technique.

Dual staining is also useful for the measurement of digital cell images. High-color-contrast images allow us to segregate bacteria more easily from nonbacterial substances, which are incorrectly recognized by a computer. Recent progress in the measurement of bacterial size has included automatic threshold determination systems (Bloem et al., 1995; Blackburn et al., 1998), which are faster than the manual threshold determination method used here. The high contrast is also helpful for the problem of dim cells, which have weak fluorescence and are difficult (or almost impossible with the automatic threshold determination system) to distinguish from the background by using only AO or DAPI.

2.4.2 Effect of dispersion and sediment characteristics

As already mentioned, although the bacterial cell counts increase when the masking effect due to aggregates is decreased by increasing the treatment time, longer dispersion times can cause cell destruction. This cell destruction can result in the formation of an unclear cell edge due to the leaking of protoplasm and can hence lead to the inaccurate measurement of the biovolume and abundance of cells. In the present study, cell destruction, which was indicated by a decline in the number of bacteria, was observed with the application of homogenization treatment but not with the ultrasonic cleaner or sonicator treatments (**Figure 4**). The homogenizer mechanically breaks down sediment particles into finer ones, resulting in increased background interference. Hence, the counting and sizing of bacteria in a homogenized sample is relatively time-consuming and somewhat subjective compared to samples treated by the other two methods. For the sonication treatment, no cell destruction has been reported (Deflaun and Mayer, 1983; Epstein and Rossel, 1995; Epstein et al., 1997). Epstein et al. (1997) showed no cell destruction in samples treated with optimal dispersing time based on the thorough examination of labeled bacteria with radioisotopes. For the ultrasonic cleaner treatment, Ellery and Schleyer (1984) reported that cell destruction occurred with a 100- to 200-W output ultrasonic cleaner but not with the 60-W output ultrasonic cleaner used here. The main reason for this discrepancy is probably the difference in the specifications and/or intensities of the ultrasonic cleaners. Therefore, there is possible cell destruction in the case of too-long or too-intense dispersion with the sonicator as well as with the ultrasonic cleaner.

For the beach sand sediment, the maximum number of dispersed bacteria was not significantly different among the three dispersion techniques (**Table 2**). However, for the sandflat and mudflat sediments, the ultrasonic cleaner yielded fewer bacteria than the other dispersion methods (**Table 2**). This indicates that for the silt- and clay-rich sediments, where the viscosity (EPS) was also higher (**Table 1**), the ultrasonic cleaner treat-

ment did not efficiently separate bacterial cells, at least with my low-power output equipment. Nonetheless, differences in the maximum yield of bacteria among the dispersion techniques were not as high as those previously reported (Epstein and Rossel, 1995).

For the homogenizer, bacterial cell counts peaked over a short dispersion time in all of the sediments, while for the ultrasonic cleaner and sonicator, the cell counts increased as the dispersion time increased and then leveled off (**Figure 4**). The pattern of cell counts during homogenization was similar to patterns previously reported (Dye, 1983; Epstein and Rossel, 1995) but somewhat different from the observations of Montagna (1982) and Ellery and Schleyer (1984), which were similar to those for the ultrasonic cleaner and sonicator. These differences are presumably due to the increased cell counts through the application of dual staining. Direct observation of samples after 0.5 to 2 min of the homogenization treatment revealed that there were significant numbers of bacteria still trapped in aggregates.

The range of bacterial biovolumes investigated was consistent with those previously reported (Rublee, 1982; Meyer-Reil, 1983; Montagna, 1984; Imai, 1987). The largest bacterial biovolumes were observed in the finest sediments. In addition, the more dispersed bacteria were observed in the finer sediments. This tendency has been found by many workers in relation to sediment grain surface area (Deflaun and Mayer, 1983; Schmidt et al., 1998), protected habitat (Weise and Rheinheimer, 1978), organic content (Deming and Baross, 1993), grazer regulation (Fenchel, 1984), and porosity (Schmidt et al., 1998) and need not be discussed further. From the number of bacterial cells and biovolumes measured, bacterial biomass can be calculated; the high number and large size of bacteria in fine sediments results in a large bacterial biomass in fine sediments.

2.4.3 Implication of bacterial biomass for nutrient cycling

Logically, one should expect a relationship between bacterial biomass and their concomitant rate and flux of nutrients; however, no studies have been conducted on this relationship except for nitrification. Reports suggest that nitrification activity in sediments is controlled by the population dynamics of nitrifying bacteria (Henriksen et al., 1981; Jenkins and Kemp, 1984; Bodelier et al., 1996), as well as by the availability of ammonium and oxygen (Fenchel et al., 1998). The biogeochemical role of bacterial biomass in sediments is better recognized in trophic links through the benthic food chain than in the transformation of matter (Alongi, 1998). Nitrogen and phosphorus comprising bacterial bodies are immobilized as a reservoir, which is then transferred to protozoans, invertebrates, and some vertebrates by grazing. Indeed, the importance of immobilized nitrogen and phosphorus pools has long been accepted when reconciling models of nutrient cycling in marine sediments (Blackburn, 1986; Nakata and Hata, 1990). Nevertheless, a better knowledge of the relationships between bacterial biomass or immobilized nutrient pools and associated nutrient transfer rates is required to understand nutrient cycling in marine sediments as a whole.

2.5 Conclusions

Dual staining has advantages over conventional staining techniques, especially for silt-, clay-, and detritus-rich sediments, by reducing serious background fluorescence. With dual staining, bacteria stand out from other objects and can hence be more easily counted and sized. Ultrasonic cleaner and sonicator treatments are recommended for dispersing bacteria from aggregates, while the homogenization treatment may cause cell destruction if applied for too long. The ultrasonic cleaner treatment, however, has the possibility of insufficient dispersion for silt- and clay-rich sediments. Small bacteria (<0.1 μm^3) require a longer dispersion time than large bacteria (>0.1 μm^3) to produce consistent maximum results. It is concluded that studies of bacterial cell size require a treatment time sufficiently long to disperse small bacteria in order to obtain a realistic size distribution.

2.6 Summary

I measured the abundance and biovolume of bacteria in intertidal sediments from Tokyo Bay, Japan, by using a dual-staining technique (4′,6-diamidino-2-phenylindole and acridine orange) and several dispersion techniques (ultrasonic cleaner, ultrasonic sonicator, and tissue homogenizer). Dual staining reduced serious background fluorescence, particularly when used for silt-, clay-, and detritus-rich sediments, and allowed us to distinguish bacteria from other objects during both counting and sizing. Within the studied samples, the number of bacterial cells ranged from 0.20×10^9 to 3.54×10^9 g of wet sediment^{-1}. With the ultrasonic cleaner and sonicator treatments, the bacterial numbers for all of the sites initially increased with dispersion time and then became constant. For the homogenizer treatments, the highest bacterial numbers were observed for the shortest (0.5- to 2-min) treatments, and the counts then declined steeply as the homogenization time increased, indicating that cell destruction occurred. The ultrasonic cleaner treatment could result in insufficient dispersion of bacteria for fine sediments. Within the studied samples, the bacterial biovolume ranged from 0.07 to 0.22 μm^3. With the ultrasonic cleaner and sonicator treatments, the biovolume peaked during the shorter dispersion time. This pattern was caused not by cell destruction but by the incremental portion of dispersed small cells. I concluded that application of the ultrasonic cleaner and sonicator treatments over longer dispersion times reflect a realistic

size spectrum and was hence preferable for accurate estimation of mean bacterial biovolumes. The findings described above can contribute to a better understanding of the role of bacterial biomass in immobilized nutrient pools and associated nutrient cycling; however, further investigations are required for a quantitative estimation of the role of immobilized nutrient pools in nutrient cycling.

3. Role of Sediment-Water Nutrient Exchanges in Intertidal Sandflats

3.1 Introduction

High nutrient loading in coastal ecosystems has recently caused serious eutrophication problems. In a eutrophic shallow environment, oxygen-depleted water is occasionally generated at the bottom of the water column due to the accumulation of organic matter (Ochi and Takeoka, 1986; Kemp et al., 1992) and can cause the death of benthic macrofauna (Rosenberg and Loo, 1988). Autochthonous nutrients from sediments as well as allochthonous nutrients from rivers can both contribute to eutrophication in coastal areas. Hence, benthic mineralization is considered to be an important pathway for nutrients in shallow water ecosystems (e.g. Blackburn and Henriksen, 1983; Kemp et al., 1992). Recycled nutrients are released from sediments to overlying waters through sediment-water exchange processes and can be taken up by phytoplankton.

Several processes have been shown to regulate the exchange of nutrients between sediment and water: (1) molecular diffusion, caused by a nutrient gradient at the sediment-water interface (Sweerts et al., 1991), (2) faunal activity, such as excretion or ventilation (Blackburn and Henriksen, 1983; Rutgers van der Loeff et al., 1984; Kristensen, 1985; Kristensen, 1988), and (3) uptake of nutrients by benthic microorganisms (Sundbäck et al., 1991; Rizzo et al., 1992; Rysgaard et al., 1995; van Duyl et al, 1993). An intertidal flat, where sufficient light penetrates to the sediment due to emersion, has characteristically high levels of benthic microalgal biomass and productivity (Colijn and de Jonge, 1984; Varela and Penas, 1985). Photosynthetic processes can result in large diurnal changes in nutrient demands and can hence primarily affect the nutrient cycle near the sediment surface.

Denitrification is also known to produce a significant nutrient sink in coastal ecosystems due to the formation of gaseous nitrogen (e.g. Kaplan et al., 1977; Koike and Hattori, 1978; Nedwell and Trimmer, 1996). The rate of sedimentary denitrification is affected by the bacterial processes associated with nitrogen cycling in marine estuaries in two ways: (1) ammonium oxidation by nitrification in the sediment is strongly coupled with denitrification (Jenkins and Kemp, 1984; Rysgaard et al., 1995; Ogilvie et al., 1997), and thus nitrification itself indirectly removes nitrogen through these coupled processes; and (2) dissimilatory nitrate reduction to ammonium competes with denitrification for nitrate as the terminal electron acceptor for respiratory electron transport (Herbert and Nedwell, 1990). The competition between denitrifier and ammonifier under anaerobic conditions consequently affects the removal of nitrogen by sedimentary denitrification.

The importance of intertidal sediments in nutrient cycling within Japanese coastal areas has been discussed (Kurihara, 1988; Sasaki, 1989); however, the quantification of nutrient fluxes is not well established. Since nutrient flux measurements were mainly conducted in subtidal areas (e.g. Sundbäck et al., 1991; Rizzo et al., 1992; Cowan et al., 1996), there is little flux data for eutrophic intertidal areas (Falcão and Vale, 1990; Asmus et al., 1998).

In this chapter, I report seasonal changes in the simultaneously measured rates of nitrification, denitrification, sediment-water nutrient exchange, and sedimentary oxygen production for the Banzu intertidal sandflat located in Tokyo Bay. These data were then used to assess the relative importance of processes on spatial and temporal variation in sediment-water nutrient exchange fluxes and denitrification in the intertidal sandflat.

3.2 Materials and Methods

3.2.1 Study site and sampling

The Banzu intertidal sandflat is located on the east coast of Tokyo Bay (Japan) and covers an area of 7.6 km^2 (**Figure 8**). Tokyo Bay receives a nutrient loading from a population of ca. 26 million humans (320 t N d^{-1} for total nitrogen and 26 t P d^{-1} for total phosphorus, Nakanishi, 1993), and is subjected to heavy eutrophication and anoxia in bottom waters over a wide area during the summer. Tides are semi-diurnal with amplitudes from 0.5 to 1.6 m (Maritime Safety Agency, 1999). The Obitsu River has a watershed area of 267 km^2 and a 2.5 to 3.0 m^3 s^{-1} of ordinal discharge. A preliminary study revealed that seawater advected by tidal movement is the major source of nitrogen although there is also an adjacent river mouth. The sampling site (35°24.2′N, 139°54.2′E) is 30 cm above mean sea level, experiencing exposure and submergence during each tidal phase. The slope of the seabed at the sampling site is very low (0.07 cm m^{-1}). Sediments are characterized by well-sorted fine sand (99.6% sand and 0.4% silt) with a median grain size of 170 μm (see **Chapter 2**). Organic carbon and total nitrogen contents per dry weight of the sediment at 0 to 20 mm depth from August 1998 to September 1999 were 0.981 ± 0.047 mg C g^{-1} (mean ± SE, n = 45) and 0.214 ± 0.013 mg N g^{-1} (mean ± SE, n = 45), respectively. There is no macro-vegetation, and

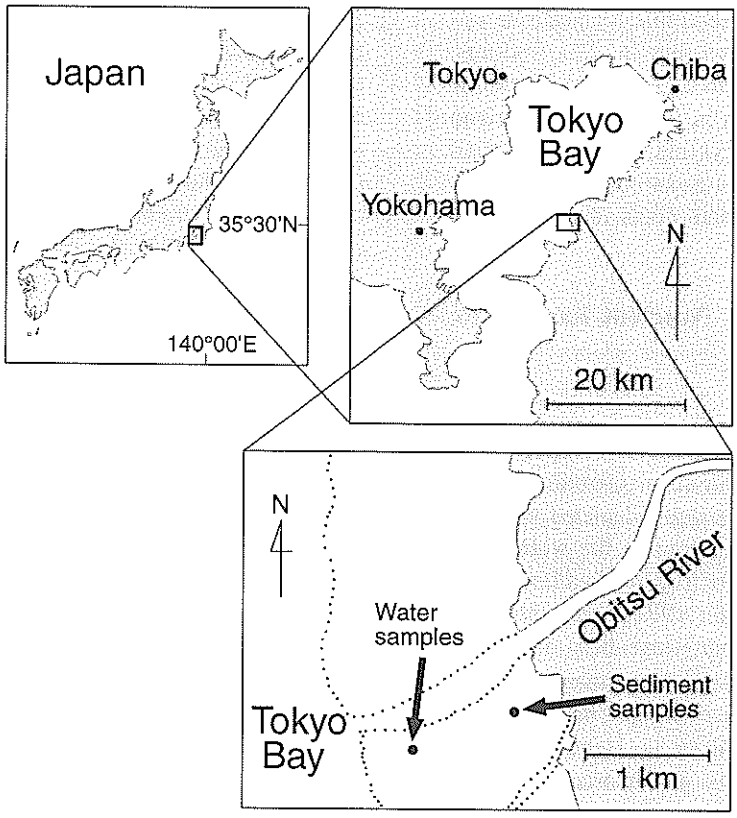

Figure 8 Location of the study site (Banzu intertidal sandflat, Tokyo Bay). Dotted line indicates the lowest tidal level. Sediment samples were taken when the sediment was exposed on the ebb tide. Water samples were taken at a lower site, which was submerged at the time of sampling.

pennate diatoms dominate the epibenthic microalgal flora.

I conducted 10 seasonal surveys during the spring tide from May 1997 to March 1999. All of the sediment samples were taken when the sediment was exposed on the ebb tide. Water samples were taken in cubitainers at a lower site, which was submerged at the time of sampling.

3.2.2 Sediment characteristics

Sediment temperature, redox potential (Eh), and nutrient profiles in the porewater were measured. Temperature was measured with a thermistor-type thermometer (RT-10; Tabai Espec) inserted into the sediment. Eh was measured in situ with a pH/mV meter (HM-14P; TOA) equipped with a platinum redox electrode.

Sediment cores (n = 3) were collected randomly from the site on the day of sampling, using an acrylic corer. Sediment cores were immediately cut in situ into 0–10 mm, 10–20 mm, 20–30 mm, 30–40 mm, 40–50 mm, and 90–100 mm segments for samples in 1997 and 0–2.5 mm, 2.5–5 mm, 5–10 mm, 10–15 mm, 15–20 mm, 20–25 mm, 25–30 mm, 30–40 mm, 40–50 mm, and 90–100 mm segments for samples in 1998. Sliced sediments were immediately fixed by dried ice in order to stop biogeochemical reactions. Fixed sediments were thawed and filled in syringes (10 ml) and then centrifuged for 10 min at 2,000 rpm (580 × g) at ambient temperature. Extracted water was filtered through a Millipore HA filter. Filtered water was immediately frozen for the later analysis of ammonium, nitrate, nitrite, and phosphate on an analyzer (TRAACS-800; Bran+Luebbe). Water obtained at the lower site was filtered and analyzed in the same way.

3.2.3 Calculation of diffusive fluxes across the sediment-water interface

The diffusive efflux of nutrient from the sediment was calculated according to Fick's first law as described by Berner (1980):

$$J = -\varphi D_S(\partial C/\partial x) \quad (2)$$

where J is the rate of efflux, φ is the sediment porosity, D_S is the diffusion coefficient, and $\partial C/\partial x$ is the concentration gradient across the sediment-water interface. The

diffusion coefficient in particle-free water was corrected for temperature (Li and Gregory, 1974) and tortuosity using the measured porosity and porosity-tortuosity relationships reported by Sweerts et al. (1991). ∂x was assumed to be 1.25 mm for all the samples (see Section 3.4.1).

3.2.4 Sediment-water nutrient exchanges

At the site, eight replicate cores of intact undisturbed sediment were taken to a depth of 20 cm using acrylic core tubes (8.6-cm internal diameter × 30-cm long), each sealed at the bottom with a rubber bung. Water collected in the cubitainers was used to fill the top 10 cm of each core tube, taking care not to disturb the surface of the sediment. Another eight replicate cores filled with only water were used as the controls. The top of each core tube was capped by an acrylic lid equipped with two ports for sampling and aeration (**Figure 9**). The cores were left one night with aeration in a water bath held at in situ water temperature to allow sediment to re-occupy the artifactual micro gaps between the core tube and the sediment.

The following morning, the water in each of the 16 core tubes was replaced with water from the cubitainer and left to reequilibrate for 1 h prior to the experiment. The water columns were aerated in order to ensure a continuous oxygen supply and stirring during the experiment. The cores were then incubated in a water bath maintained at in situ temperature with half of the cores (four sediment and four control cores) being exposed to sunlight, and the other half darkened. The photon flux of photosynthetically available radiation (PAR) was continuously measured during the experiment using a Biospherical quantum sensor.

Nutrient samples were taken four times within a period of 7 h. The exchange rate of nutrients was estimated from the rate of linear change in concentration calculated by a regression analysis during the incubation period. If no significant regression was found ($P > 0.05$), the rate was considered to be zero. The rates of change in the water column control cores were then subtracted from the rates of change in the sediment cores.

After the experiment, the sediment in each core was sieved (1 mm mesh) to retain macrofauna. Macrofauna were preserved in 10% formalin-seawater solution buffered with sodium borate and stored for later counting. In addition, the upper 1 cm of the sediment in each core was used for the analysis of photosynthetic pigments, extracted using 90% acetone solution, spectrophotometrically analyzed (U-3200; Hitachi) according to Lorenzen (1967).

3.2.5 Nitrification

The rate of nitrification was obtained by measuring the change in the nitrite concentration in the sediment

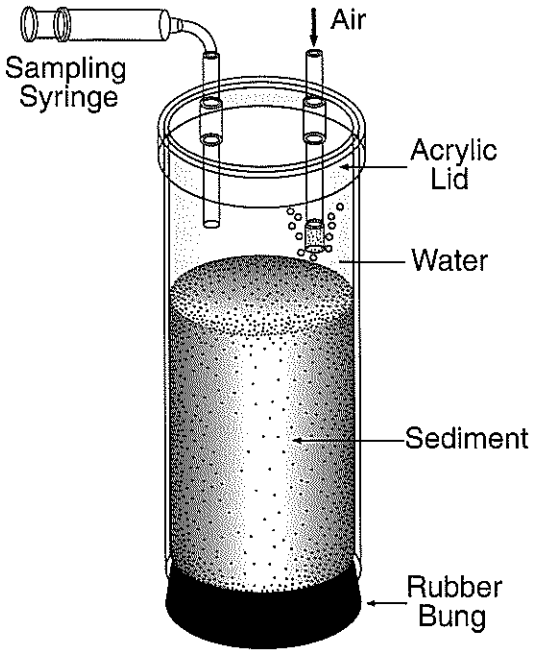

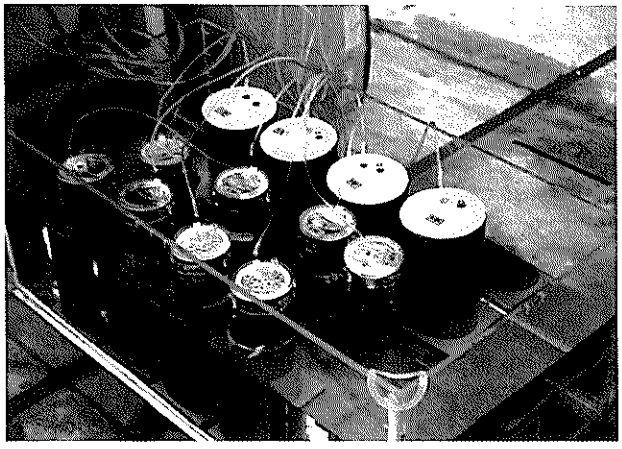

Figure 9 Schematic diagram and photo of the incubation core used in the experiment to measure sediment-water nutrient exchanges

samples containing allylthiourea (ATU) or sodium chlorate ($NaClO_3$), which were used to inhibit the oxidation of ammonium and nitrite, respectively (Bianchi et al., 1994; Gilbert et al., 1997). The water collected from the sampling site was filled into six sets of triplicate flasks (200 ml). Two triplicate sets of flasks received ATU to a final concentration of 10 mg liter^{-1}, two received 10 mM $NaClO_3$ while the others served as controls. The upper 5 cm of the sediment was divided into subsamples (6 g wet) and added to one to two sets of the control, ATU, and $NaClO_3$ flasks. The subsamples were thoroughly mixed with the water and incubated at in

situ temperature. The concentration of nitrite was measured every 3 h from zero time to 9 h. At the time of sampling, the flasks were vigorously shaken and 5 ml samples were taken and analyzed. The rate of nitrification was calculated from the data obtained during the linear nitrite production or consumption phases. If no significant correlation was found ($P > 0.05$), the rate was considered to be zero. The rate was expressed in μmol N m^{-2} h^{-1} (range of sediment depth: 0 to 5 cm) using the wet density of the sediment samples. The experiment was performed within 24 h of sampling.

3.2.6 Denitrification

An acetylene inhibition technique was used to assay for denitrification. This method measures the accumulation of nitrous oxide since acetylene inhibits the reduction of nitrous oxide to dinitrogen (Balderston et al., 1976; Koch et al., 1992; Joye and Paerl, 1993). The sample water (30 ml) saturated with acetylene was placed in each of the five replicate 60 ml gas-tight vials. The sediment subsamples (5 g) were added to the vials. The vials were placed on a shaker for 10 min, then incubated at ambient temperature. Nitrous oxide concentrations of headspace gas were determined by gas chromatography (GC-14B; Shimadzu) with an electron capture detector at time zero and after 6 h of incubation. The rate of denitrification was estimated by calculating the rate of change in the concentration of nitrous oxide during incubation. The experiment was performed within 24 h of sampling.

3.2.7 Oxygen production

At the site, triplicate sediment cores were taken to a depth of 20 cm using acrylic core tubes (4.5-cm internal diameter × 30-cm long). Core samples were left in the laboratory in the same way as in the nutrient exchange experiment previously described. The following morning, the water in the cores was replaced with the water from the cubitainer and left to reequilibrate. The top of each core was completely capped to exclude air bubbles, and the cores were incubated in a water bath. The concentration of dissolved oxygen in the water was measured with an oxygen electrode (No. 5730; YSI) inserted in each core tube. The water in the cores was stirred by the electrode itself. Data were monitored every 5 min for 1 h. The rates of change in the dissolved oxygen concentration were statistically analyzed for linearity with respect to time. At the end of the experiment, chlorophyll *a* in the upper 1 cm of the sediment in each core was analyzed in the same way.

3.2.8 Soft tissue dry weight/total live weight ratio for bivalves

To convert the total live weight of the bivalve *Ruditapes philippinarum* into the dry weight biomass, a total of 92 individuals of *R. philippinarum* were collected randomly during different seasons from the sampling site. In the laboratory, the total live weight of each animal collected was determined. After this operation, the soft tissues of each animal were removed from the shell, dried at 60°C for 48 h and weighed again (dry weight). A linear equation describing the plots of soft tissue dry weight versus total live weight was obtained from all of the samples (**Figure 10**). This equation was used to calculate the dry weight biomass of *R. philippinarum* collected from the core samples.

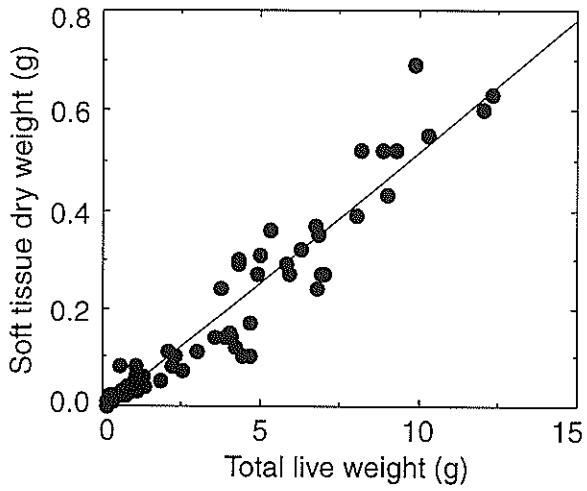

Figure 10 Relationship between soft tissue dry weight (g) and total live weight (g) for *Ruditapes philippinarum* (linear regression line: $y = 0.0507x$, $r^2 = 0.93$; $n = 92$)

3.2.9 Statistical analysis

Linear regression was used to examine the relationship between nutrient exchange fluxes and the soft tissue dry weight of *R. philippinarum*. A one-way ANOVA was used to examine statistical differences in nutrient exchange fluxes between light conditions and between seasons. Each ANOVA was followed by a SNK test of means. Data sets were tested for homogeneity of variances (Hartley test), and the log-transformed values were used if needed for a normal distribution.

3.3 Results

3.3.1 Sediment characteristics

Mean sediment temperature in the top 10 cm ranged from 7.4 to 30.1°C on the day of sampling (**Table 4**). Mean Eh showed >0 mV for all seasons, with the lowest values recorded in summer, when the mean sediment temperature was maximal. Higher macrofaunal densities were observed at the Banzu intertidal sandflat (**Table 5**); the polychaete *Armandia* sp. and the bivalve *Ruditapes*

Table 4 Environmental parameters on the sampling day and at incubation

	Sampling		Incubation				
	Temp[a] (°C)	Eh[a] (mV)	Temp[b] (°C)	PAR[c] (μmol m^{-2} s^{-1})	Chl *a*[d] (μg g^{-1} wet)	Pheo[d] (μg g^{-1} wet)	Total pigm[d] (μg g^{-1} wet)
May 97	—	—	23.1	—	1.01 ± 0.20	2.70 ± 0.17	3.71 ± 0.29
Jul 97	25.7	60	25.8	444	1.12 ± 0.20	2.26 ± 0.19	3.37 ± 0.19
Sep 97	26.7	114	25.3	281	0.83 ± 0.20	1.90 ± 0.24	2.73 ± 0.27
Nov 97	16.8	213	17.2	41	0.30 ± 0.08	1.08 ± 0.15	1.37 ± 0.09
Feb 98	7.4	255	12.4	610	3.92 ± 0.46	4.86 ± 0.45	8.78 ± 0.74
May 98	20.9	108	21.3	656	4.02 ± 0.24	2.95 ± 0.22	6.97 ± 0.33
Jul 98	—	99	27.2	321	4.81 ± 0.89	2.61 ± 0.33	7.42 ± 1.04
Sep 98	30.1	29	28.4	583	5.21 ± 0.22	3.65 ± 0.31	8.86 ± 0.51
Nov 98	24.2	294	21.3	242	4.32 ± 0.40	1.65 ± 0.17	5.97 ± 0.51
Mar 99	17.9	272	12.8	250	1.54 ± 0.32	3.57 ± 0.49	5.12 ± 0.65

[a]Temp and Eh, mean sediment temperature and redox potential in the top 10 cm, respectively. These were measured during the exposed period from ca. 10:00 to 13:00.

[b]Temp, water temperature controlled during incubation.

[c]PAR, mean photosynthetically available radiation measured throughout the incubation period.

[d]Chl *a*, Pheo, and Total pigm, chlorophyll *a*, pheopigments, and chlorophyll *a* + pheopigments in the top 1 cm (mean ± SE), respectively.

Table 5 Total densities (mean ± SE) and dominant species of macrofauna (%) at the sampling site (depth: 0–20 cm)

	Total (individuals m^{-2})	Dominated macrofauna			
		R. philippinarum[a]	*Armandia* sp.	Other polychaetes[b]	*B. cumingii*[a]
May 97	4541 ± 673	66.8	0.0	26.1	5.7
Jul 97	2647 ± 223	65.0	0.0	30.1	0.0
Sep 97	5466 ± 914	38.6	60.2	0.0	0.0
Nov 97	4584 ± 943	70.0	4.7	20.2	0.0
Feb 98	1657 ± 232	5.2	48.1	33.8	0.0
May 98	—	—	—	—	—
Jul 98	6886 ± 775	3.8	10.6	79.4	0.0
Sep 98	3658 ± 753	13.5	0.0	55.9	16.5
Nov 98	3163 ± 187	16.3	0.0	37.4	23.8
Mar 99	5186 ± 559	8.7	41.9	0.0	13.3

[a]*R. philippinarum* and *B. cumingii*, the bivalve *Ruditapes philippinarum* and the gastropod *Batillaria cumingii*, respectively.

[b]Percentages of total polychaetes except for *Armandia* sp.

philippinarum dominated infauna, whereas the gastropod *Batillaria cumingii* dominated epifauna.

3.3.2 Nutrient concentration profiles and diffusive fluxes

Depth profiles of porewater nitrate + nitrite (hereafter, nitrate) and phosphate showed marked concentration gradients with depth during emersion (**Figure 11**). Nitrate and phosphate concentrations peaked in the uppermost layer of sediments for all seasons, and below this they sharply declined until a depth of 30 mm. Mean nitrate concentrations in the top 10 mm layer peaked in winter and were lowest in summer (**Table 6**). The

profile of ammonium concentration exhibited a gradual increase from the sediment-water interface in summer; in contrast, during other seasons the pattern of ammonium concentration was either stable or gradually decreased with increasing depth (**Figure 11**). All the nutrient concentrations in the uppermost layer of sediments, except for nitrate in September 98, were always much higher than those in the overlying waters (**Table 6**).

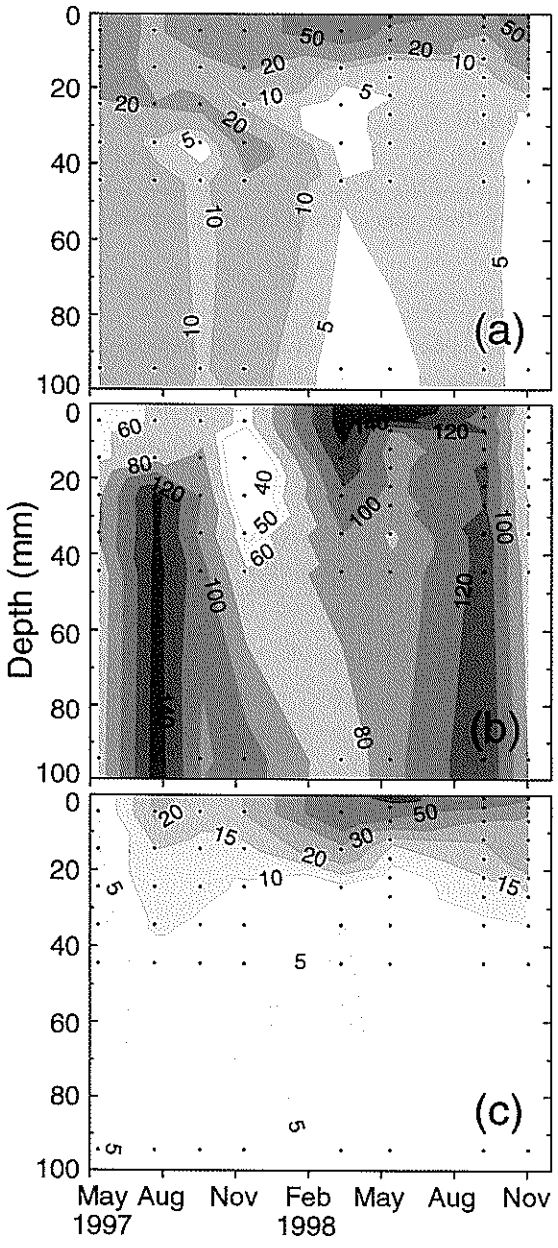

Figure 11 Mean concentrations (μM) (n = 3) of porewater nitrate (a), ammonium (b), and phosphate (c). Contour plots were determined using a linear interpolation method.

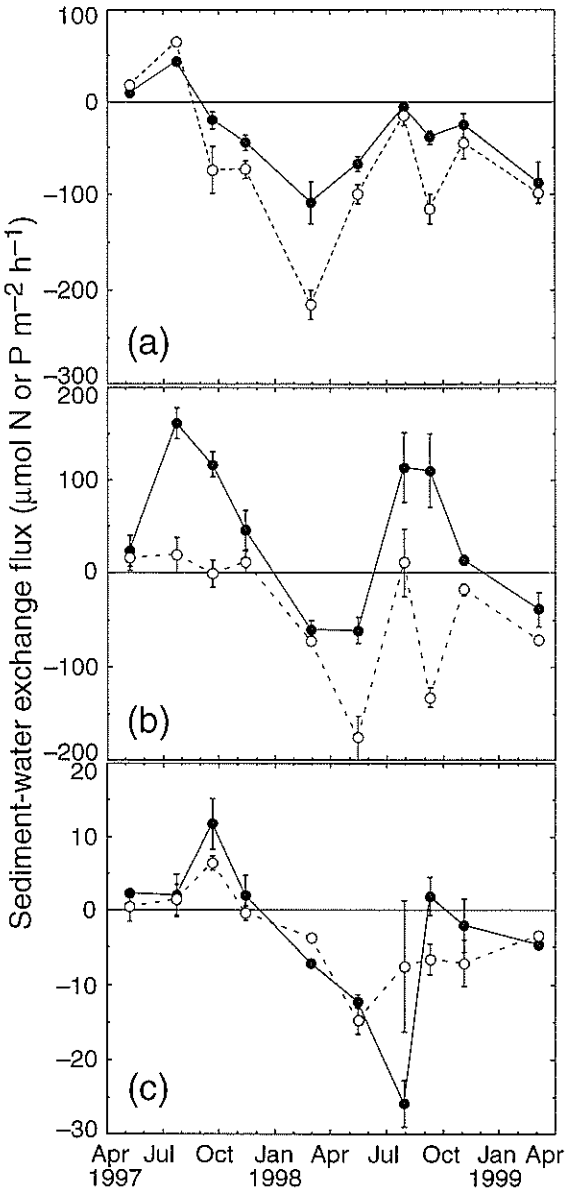

Figure 12 Measured nitrate + nitrite (a), ammonium (b), and phosphate (c) exchange fluxes (μmol N or P m^{-2} h^{-1}) across the sediment-water interface in the light (○) and dark (●). Positive values indicate effluxes from the sediment. Bars indicate standard errors (n = 4).

This contrast resulted in great diffusive effluxes from the sediment, ranging from –4.0 to 59.5 μmol N m^{-2} h^{-1} for nitrate, 63.4 to 268.1 μmol N m^{-2} h^{-1} for ammonium, and 1.3 to 17.0 μmol P m^{-2} h^{-1} for phosphate.

3.3.3 Sediment-water nutrient exchanges

High PAR values (242 to 656 μmol m^{-2} s^{-1}) were recorded for all cases except for those measured in November 1997 (41 μmol m^{-2} s^{-1}) (**Table 4**). The chloro-

Table 6 Diffusive fluxes (Diff) across the sediment-water interface. Positive values indicate effluxes from the sediment.

	$NO_3^- + NO_2^-$			NH_4^+			PO_4^{3-}		
	Pw[a]	Ow[b]	Diff[c]	Pw	Ow	Diff	Pw	Ow	Diff
May 97	29.7	2.5	34.8	54.0	1.4	70.1	4.2	0.6	1.3
Jul 97	17.5	5.9	17.1	61.3	6.2	84.6	21.5	3.5	9.0
Sep 97	38.0	18.0	28.5	74.1	10.3	94.0	17.2	1.7	7.2
Nov 97	39.8	14.9	29.2	53.4	2.1	63.4	20.2	1.1	3.7
Feb 98	99.4	25.1	22.0	131.4	5.0	161.5	59.9	0.6	1.6
May 98	65.9	13.1	11.6	89.8	12.1	268.1	48.6	2.5	8.2
Sep 98	17.0	21.6	–4.0	131.6	17.3	79.3	37.6	3.0	17.0
Nov 98	47.6	9.9	59.5	41.5	2.1	63.4	23.6	1.9	7.7

[a]Pw, mean porewater nutrient concentration in the top 10 mm layer, expressed in μM (n = 3 from May 97 to Nov 97; n = 9 for the others).
[b]Ow, overlying water nutrient concentration (μM).
[c]Expressed in μmol N or P m^{-2} h^{-1}.

phyll *a* content in the top 10 mm of sediments did not exhibit a clear seasonal fluctuation, ranging from 0.30 ± 0.08 to 5.21 ± 0.22 μg g of wet sediment^{-1} (mean ± SE) within the studied samples (**Table 4**).

The measured nitrate exchange fluxes ranged from –215.0 ± 15.8 to 65.2 ± 4.4 μmol N m^{-2} h^{-1} (mean ± SE) in the light and from –108.0 ± 22.1 to 43.4 ± 3.6 μmol N m^{-2} h^{-1} (mean ± SE) in the dark (**Figure 12**). The sediment samples all acted as sinks for nitrate except for the samples collected in May 1997 and July 1997. The mean uptake rate of nitrate by the sediment was higher in the light (–65.3 μmol N m^{-2} h^{-1}) than in the dark (–34.6 μmol N m^{-2} h^{-1}) throughout the studied period. The one-way ANOVA revealed four cases of nitrate exchange where there was a significant difference between samples subjected to different light conditions (P < 0.05) (**Table 7**). The measured ammonium exchange fluxes ranged from –176.2 ± 23.6 to 18.9 ± 18.9 μmol N m^{-2} h^{-1} (mean ± SE) in the light and from –60.6 ± 13.6 to 161.5 ± 16.7 μmol N m^{-2} h^{-1} (mean ± SE) in the dark (**Figure 12**). The sediment samples mainly acted as sinks for ammonium when exposed to light. The mean uptake rate of ammonium by the sediment was markedly higher in the light (–41.1 μmol N m^{-2} h^{-1}) than in the dark (42.5 μmol N m^{-2} h^{-1}) throughout the studied period. The one-way ANOVA showed there were five cases of ammonium exchange where a statistical difference is recognized between light and dark conditions (P < 0.05) (**Table 7**). The SNK test showed that the efflux of ammonium for samples under dark conditions during the summer period was significantly higher than during any other season (P < 0.05) (**Table 8**). The measured phosphate exchange fluxes ranged from –14.7 ± 1.7 to 6.4 ± 1.0 μmol P m^{-2} h^{-1} (mean ± SE) in the light and from –25.9 ± 3.1 to 11.7 ± 3.5 μmol P m^{-2} h^{-1} (mean ± SE) in the dark (**Figure 12**). Most of the sediment samples acted as sinks for phosphate under both light and dark conditions. The mean uptake rate of phosphate by the sediment was slightly higher in the light (–3.5 μmol P m^{-2} h^{-1}) than in the dark (–3.2 μmol P m^{-2} h^{-1}) throughout the studied period. The one-way ANOVA revealed only two cases of phosphate exchange fluxes that is significantly different between light and dark conditions (P < 0.05) (**Table 7**).

Table 7 Significance level of difference in the sediment-water nutrient exchange fluxes between light/dark treatments

	$NO_3^- + NO_2^-$	NH_4^+	PO_4^{3-}
May 97	NS[a]	NS	NS
Jul 97	0.009	0.001	NS
Sep 97	NS	0.001	NS
Nov 97	NS	NS	NS
Feb 98	0.008	NS	0.001
May 98	0.040	0.005	NS
Jul 98	NS	NS	NS
Sep 98	0.005	0.001	NS
Nov 98	NS	0.009	NS
Mar 99	NS	NS	0.041

[a]NS, not significant (P > 0.05).

Table 8 Multiple comarison (SNK test) of the sediment-water nutrient exchange fluxes between sampling days

	Treatment	Significance at 5% level[a]
$NO_3^- + NO_2^-$	Light	Feb98 < Sep98 Mar99 May98 Sep97 Nov97 Nov98 Jul98 May97 < Jul97
	Dark	Feb98 Mar99 May98 Nov97 Sep98 Nov98 Sep97 Jul98 May97 Jul97
NH_4^+	Light	May98 Sep98 < Feb98 Mar99 < Nov98 Sep97 Jul98 Nov97 May97 Jul97
	Dark	May98 Feb98 Mar99 Nov98 May97 Nov97 < Sep98 Jul98 Sep97 Jul97
PO_4^{3-}	Light	May98 Jul98 Nov98 Sep98 Feb98 Mar99 Nov97 May97 Jul97 Sep97
	Dark	Jul98 < May98 Feb98 Mar99 Nov98 Sep98 Jul97 Nov97 May97 Sep97

[a]Underlining indicates a statistically homogenous group.

3.3.4 Microphytobenthic productivity and nitrogen uptake

In September 1997, the measured oxygen consumption rate was 62.4 ± 2.1 mg O_2 m^{-2} h^{-1} (mean ± SE) in the dark. In the light, the measured oxygen production rate was 89.5 ± 15.9 mg O_2 m^{-2} h^{-1} (mean ± SE). Thus, microphytobenthic gross primary production was estimated to be 151.9 ± 17.1 mg O_2 m^{-2} h^{-1}. The uptake of nitrogen by benthic microalgae, calculated from the gross oxygen productivity assuming a Redfield C:N ratio of 106:16 (Redfield et al., 1963; Hillebrand and Sommer, 1999) and a photosynthetic quotient of 1.25 (Williams et al., 1979), was estimated to be 573.4 ± 64.4 μmol N m^{-2} h^{-1}.

3.3.5 Nitrification and denitrification

In September 1997, the measured ammonium and nitrite oxidation rates were 84.9 ± 4.1 and 46.0 ± 3.8 μmol N m^{-2} h^{-1} (mean ± SE), respectively. The ammonium oxidation rate was significantly higher than the nitrite oxidation rate in the top 5 cm of the sediment ($P < 0.001$). The measured denitrification rate was 99.6 ± 23.5 μmol N m^{-2} h^{-1} (mean ± SE) and was not significantly different from the ammonium oxidation rate ($P > 0.05$).

3.4 Discussion

3.4.1 Effect of diffusive fluxes on total sediment-water nutrient exchange

The diffusive nutrient fluxes calculated here (**Table 6**) showed their remarkable contribution to the total exchange flux at the sediment-water interface (see **Figure 12**). This is attributed to both (1) the large differences in nutrient concentration between the porewater and the overlying water; and (2) the better resolution of the obtained nutrient concentration profiles with depth (∂x) near the surface sediment. The diffusive flux, calculated according to Fick's first law, is dependent on ∂x (see Section 3.2.3). For all of the nutrient concentration profiles measured in 1998 (∂x = 1.25 mm), a peak in concentration was observed in the topmost layer of the sediment within the top 10 mm (**Figure 11**). In addition, similar patterns have been obtained from other shallow water sediments (Vidal and Morguí, 1995; Rocha, 1998; Yamamuro and Koike, 1998). Therefore, I extrapolated a ∂x value of 1.25 mm for the calculation of the diffusive fluxes in 1997; however, this might lead to some errors. Moreover, dense macrofaunal populations at the sampling site (**Table 5**) indicate that porosity may be underestimated due to bioturbation. The diffusive fluxes reported by other researchers have been mostly estimated from nutrient profiles with poorer depth resolution (2.5 to 10 mm), often resulting in much lower values than the total exchange fluxes (e.g. Cal-

Table 9 Linear regression ($y = ax + b$) showing the relationship between nutrient exchange fluxes (μmol N or P m^{-2} h^{-1}) (y) and soft tissue dry weight of *R. philippinarum* (g dry wt m^{-2}) (x)

		Light			Dark		
		a	b	r^2	a	b	r^2
NH_4^+	Jul 97	1.07	−7.5	0.998	9.35	80.7	0.686
	Sep 97	4.95	−107.2	0.635	7.95	−50.0	0.996
	Nov 97	0.93	−15.1	0.912	1.99	−26.3	0.990
	Jul 98	—	—	—	9.25	51.1	0.859
	Sep 98	2.82	−101.9	0.964	7.28	3.3	0.974
	Nov 98	1.07	−25.2	0.861	—	—	—
PO_4^{3-}	May 97	0.47	1.0	0.857	—	—	—
	Sep 97	0.39	−2.1	0.903	0.42	7.6	0.949
	Nov 97	0.06	−3.2	0.945	0.23	−5.2	0.895
	Jul 98	—	—	—	0.70	−30.6	0.721
	Sep 98	0.46	−10.3	0.966	0.44	−1.9	0.736
	Nov 98	0.30	−7.3	0.998	—	—	—

[a]Only equations having a high coefficient of determination ($r^2 > 0.6$) are shown.

lender and Hammond, 1982; Rutger van der Loeff et al., 1984; Kuwae et al., 1998; Magni et al., 2000). For example, the nutrient flux measured in situ with a benthic chamber has been shown to be 1 to 10 times greater than the flux calculated from porewater profiles in the Potomac River estuary (Callender and Hammond, 1982), and 2 to 10 times greater in Gullmarsfjorden (Rutger van der Loeff et al., 1984). Nevertheless, adequate depth resolution is particularly important in measuring nutrient concentration profiles when such profiles peak in the topmost sediments, as I have found for nitrate and phosphate measured during the present study.

The variability of the measured exchange flux could not be explained solely by the diffusive flux. Other release and uptake processes may cause the difference between the calculated diffusive flux and the directly measured exchange flux. Nutrient release processes can include excretion by bivalves (Blackburn and Henriksen, 1983; Magni et al., 2000) or ventilation between porewater and the water column by polychaetes (Kristensen, 1985). Kristensen (1988) reported that the population of burrow systems (macrofaunal density: 20 to 6,000 ind. m^{-2}) generate 17 to 90% of the total ammonium flux in coastal sediments. Furthermore, macrofaunal turbation may promote mixing of porewater with the overlying water, resulting in stimulation of nutrient release from sediments. Nutrient uptake processes, in turn, can include assimilation of nutrients by microbes (Cammen, 1991). The influence of these release and uptake processes on spatial and temporal variations in nutrient exchange fluxes will be discussed in the next two sections.

3.4.2 Spatial variability of measured nutrient fluxes

I compared the nutrient flux data within the replicated cores obtained on the same sampling days ($n = 4$) in order to investigate spatial variability of the measured sediment-water exchange fluxes. A linear regression analysis was performed using the macrofaunal density and photosynthetic pigment content (chlorophyll *a* and pheopigments) as independent variables, and the exchange fluxes of three nutrient species (nitrate, ammonium, and phosphate) as dependent variables (**Table 9**). A significant positive correlation between the nutrient release flux (ammonium and phosphate) and the abundance of the bivalve *Ruditapes philippinarum* (as measured by soft tissue dry weight) was found for several cases whereas the other variable pairs did not show a reliable relationship (not shown). These results can be explained by bioturbation and/or excretion of nutrients by *R. philippinarum*. If the effect of bioturbation is great, this should stimulate the release of all nutrient species from the sediment since porewater nutrient concentrations were always higher than in the overlying water, except for nitrate in September 1998 (**Table 6**). However, no relationship was found between the nitrate flux and the abundance of *R. philippinarum*. Therefore,

it is concluded that the spatial variability found for the fluxes of ammonium and phosphate was mainly attributed to excretion by *R. philippinarum*.

The slope of the linear regression (*a*) shown in **Table 9** can be assumed to express the excretion rates of *R. philippinarum*, ranging from 0.93 to 9.35 μmol N g^{-1} dry wt h^{-1} for ammonium and from 0.06 to 0.70 μmol P g^{-1} dry wt h^{-1} for phosphate. These estimated rates were comparable to those measured in Moss Landing, USA (Mann, 1979) and in Marennes-Oléron, France (Goulletquer et al., 1989) for ammonium and were at the lower level of those measured in Seto Inland Sea, Japan, for both ammonium and phosphate (Magni et al., 2000).

Ammonium and phosphate excretion rates appeared to be temperature dependent (**Figure 13**). Higher ammonium excretion rates were observed in the light than in the dark; however, the explanation for this needs further investigations. Indeed, Mukai (1993) reported that the filtration activity of *R. philippinarum* was higher in the dark; in contrast, Magni et al. (2000) showed a higher ammonium excretion rate for *R. philippinarum* in the light.

Using the curves in **Figure 13** and the data on *R. philippinarum* abundance, I calculated areal excretion fluxes for this bivalve under both light and dark conditions (**Table 10**). The calculated ammonium and phosphate excretion fluxes peaked in September 1997 under dark conditions and were lowest in February 1998 under light conditions, ranging from 0.3 ± 0.2 to 140.6 ± 12.2 μmol N m^{-2} h^{-1} (mean ± SE) for ammonium and from 0.03 ± 0.02 to 9.17 ± 0.79 μmol P m^{-2} h^{-1} (mean ± SE) for phosphate. The mean excretion fluxes of ammonium (49.0 μmol N m^{-2} h^{-1}) and phosphate (3.53 μmol P m^{-2} h^{-1}) in the dark were 61% and 50% of the mean diffusive fluxes from the sediment, respectively (**Table 6**); however, the excretion fluxes in the dark for the summer of 1997, when the bivalve densities were high, exceeded the estimated diffusive fluxes.

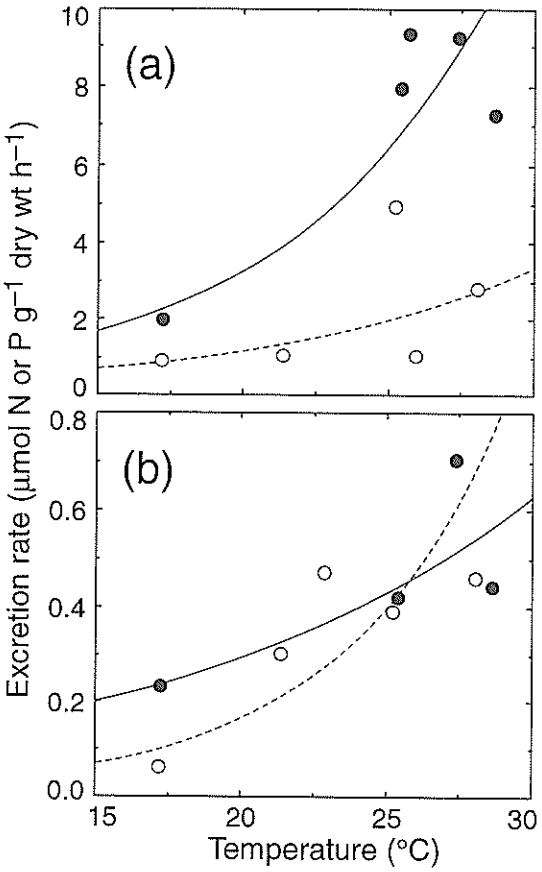

Figure 13 Temperature (°C) dependence of estimated ammonium (a) and phosphate (b) excretion rates (μmol N or P g^{-1} dry wt h^{-1}) for *Ruditapes philippinarum* under both light (○) and dark (●) conditions. Exponential regression was used for each case: $y = a \exp(bx)$. Coefficients for ammonium in light: $a = 0.141$, $b = 0.106$, $r^2 = 0.38$; in dark: $a = 0.220$, $b = 0.135$, $r^2 = 0.85$; and for phosphate in light : $a = 0.00478$, $b = 0.177$, $r^2 = 0.72$; in dark: $a = 0.06558$, $b = 0.075$, $r^2 = 0.74$.

3.4.3 Temporal variability of measured fluxes

Remarkable temporal variability was found for the measured nutrient fluxes (**Figure 12**). Peason's correlation analyses showed that all of the nutrient exchange fluxes significantly correlated with several different parameters (**Table 11**); for instance, the nitrate flux correlated positively with temperature and negatively with the pheopigments in the sediment and the concentrations of nitrate and ammonium in the overlying water. However, these results may be influenced by inter-correlation between parameters. To exclude such an effect, I performed partial correlation analyses (**Table 12**).

Partial correlation analyses revealed that all of the nutrient fluxes are strongly dependent on the associated nutrient concentrations in the overlying water under the light and that nitrate and phosphate fluxes are also dependent on the associated nutrient concentrations also under the dark. This can be attributed to concentration dependence of (1) assimilation of ammonium and phosphate by microphytobenthos and, to lesser extent, by bacteria (Cammen, 1991); and (2) dissimilatory transformation processes of nitrate by nitrate-reducing bacteria. However, a simple question arises when interpreting the results for ammonium and phosphate fluxes: why do these microbes dare to use low-concentration-nutrients in the overlying water? That is to say, why do not these benthic microbes only utilize nutrients derived from the nutrient-rich sediment? The reason for this cannot be understood from the present study; however, this curious

Table 10 Estimated areal excretion fluxes for *Ruditapes philippinarum* under both light and dark conditions

		Abund of *R.*[a]	Excretion rate[b]		Areal Excretion flux[c]	
			Light	Dark	Light	Dark
NH_4^+	May 97	2.2 ± 0.3	1.6	5.1	3.5 ± 0.5	11.2 ± 1.5
	Jul 97	16.7 ± 8.8	2.2	7.1	36.8 ± 19.3	117.9 ± 61.9
	Sep 97	20.7 ± 1.8	2.0	6.8	42.2 ± 3.6	140.6 ± 12.2
	Nov 97	32.2 ± 7.4	0.9	2.3	28.1 ± 6.5	72.4 ± 16.8
	Feb 98	0.6 ± 0.4	0.5	1.2	0.3 ± 0.2	0.8 ± 0.5
	May 98	ND[d]	1.3	3.9	ND	ND
	Jul 98	3.5 ± 2.1	2.5	8.8	8.7 ± 5.3	31.2 ± 18.9
	Sep 98	3.7 ± 1.8	2.8	10.5	10.1 ± 4.9	38.4 ± 18.6
	Nov 98	7.0 ± 3.1	1.4	3.8	9.5 ± 4.2	26.9 ± 11.8
	Mar 99	1.5 ± 0.7	0.5	1.2	0.8 ± 0.4	1.9 ± 0.9
	Mean	9.8 ± 2.9	1.6	5.1	15.6 ± 5.0	49.0 ± 15.9
PO_4^{3-}	May 97		0.27	0.38	0.60 ± 0.08	0.83 ± 0.11
	Jul 97		0.47	0.45	7.85 ± 4.12	7.57 ± 3.97
	Sep 97		0.41	0.44	8.55 ± 0.74	9.17 ± 0.79
	Nov 97		0.10	0.24	3.22 ± 0.75	7.70 ± 1.78
	Feb 98		0.04	0.17	0.03 ± 0.02	0.11 ± 0.07
	May 98		0.21	0.33	ND	ND
	Jul 98		0.57	0.51	2.00 ± 1.21	1.81 ± 1.10
	Sep 98		0.68	0.56	2.51 ± 1.21	2.07 ± 1.00
	Nov 98		0.21	0.32	1.46 ± 0.64	2.26 ± 0.99
	Mar 99		0.05	0.17	0.07 ± 0.03	0.26 ± 0.12
	Mean		0.30	0.36	2.92 ± 0.98	3.53 ± 1.10

[a]Abund of *R.*, soft tissue dry weight of *R. philippinarum* (g dry wt m^{-2}) (mean ± SE, n = 8).
[b]Excretion rate, estimated excretion rate of *R. philippinarum* (μmol N or P g^{-1} dry wt h^{-1}) calculated using the equation described in **Figure 13**.
[c]Estimated as: Abund of *R.* × Excretion rate. Values are expressesed in μmol N or P m^{-2} h^{-1} (mean ± SE, n = 8).
[d]ND, not determined.

mechanism, 'filter effect' by benthic microbes, has also been reported for other shallow water environments (e.g. Sundbäck et al., 1991). On the other hand, the nitrate flux can be interpreted as the result of nitrate being directly used for denitrification (Rysgaard et al., 1995; Ottosen et al., 2001) or dissimilatory ammonification.

The positive relationship between the abundance of *R. philippinarum* and the release flux of ammonium from the sediment suggests that bivalve excretion mediates the temporal variability of the ammonium flux (see **Table 10**). The fact that the ammonium flux was dependent on temperature only under the dark conditions may reflect the regulation of ammonium fluxes by bivalve excretion as the bivalve excretion rate was much higher under dark conditions in high temperature environments (**Figure 13**).

Some measurements of the sediment-water exchange fluxes showed that light conditions significantly affect the flux of nutrients (**Table 7**). This indicates a strong uptake of nutrients by benthic microalgae in the presence of sunlight, as has been reported for the samples of other sandy sediments (Rizzo, 1990; Sundbäck et al., 1991; Rizzo et al., 1992; Reay et al., 1995; Rysgaard et al., 1995). Preferential uptake of ammonium rather than nitrate has been reported for benthic microalgae as well as phytoplankton (Thornton et al., 1999; Cabrita and Brotas, 2000). Also in the present study, the correlation between ammonium flux and ammonium concentration

Table 11 Peason's correlation analysis of nutrient exchange fluxes and selected variables under both light and dark conditions

		Light[a]			Dark[a]		
		NO_X	NH_4^+	PO_4^{3-}	NO_X	NH_4^+	PO_4^{3-}
Overlying water[b]	NO_X	–0.817**	–0.501**	–0.051	–0.792**	–0.445**	0.065
	NH_4^+	–0.354*	–0.662**	–0.310	–0.097	0.212	–0.154
	PO_4^{3-}	0.291	–0.081	–0.486**	0.443**	0.552**	–0.539**
Sediment[c]	Temp	0.561**	0.135	0.030	0.667**	0.711**	0.036
	Chl. *a*	–0.287	–0.534**	–0.596**	–0.351*	–0.211	–0.460**
	Pheo	–0.478**	–0.416**	–0.212	–0.485**	–0.317*	–0.322*
	R. phil	0.182	0.435**	0.289	0.098	0.372**	0.349*
	Polych	–0.060	–0.128	0.073	–0.265	–0.026	–0.039

[a]*: $P < 0.05$ and **: $P < 0.01$, respectively. Release fluxes from the sediment (μmol N or P m^{-2} h^{-1}) were treated as positive variables.
[b]Overlying water, overlying water nutrient concentration (μM).
[c]Temp, Chl. *a*, Pheo, *R. phil*, and Polych, temperature (°C), chlorophyll *a* (μg g^{-1} wet), pheopigments (μg g^{-1} wet), abundance of *R. philippinarum* (g wet m^{-2}), and abundance of polychaete (g wet m^{-2}), respectively.

Table 12 Partial correlation analysis of nutrient exchange fluxes and selected variables under both light and dark conditions

		Light[a]			Dark[a]		
		NO_X	NH_4^+	PO_4^{3-}	NO_X	NH_4^+	PO_4^{3-}
Overlying water[b]	NO_X	–0.681**	0.069	—	–0.598**	0.442**	—
	NH_4^+	0.469*	–0.525**	—	—	—	—
	PO_4^{3-}	—	—	–0.481**	0.022	0.307	–0.535**
Sediment[c]	Temp	–0.252	—	—	0.210	0.459**	—
	Chl. *a*	—	0.125	–0.110	–0.235	—	–0.200
	Pheo	—	0.069	—	–0.161	0.161	–0.111
	R. phil	—	0.368*	0.029	—	0.617**	0.290
	Polych	—	—	—	—	—	—

[a]*: $P < 0.05$ and **: $P < 0.01$, respectively. Release fluxes from the sediment (μmol N or P m^{-2} h^{-1}) were treated as positive variables. All the statistically significant variables ($P < 0.05$) in **Table 11** were controlled for the calculation of coefficients.
[b]Overlying water, overlying water nutrient concentration (μM).
[c]Temp, Chl. *a*, Pheo, *R. phil*, and Polych, temperature (°C), chlorophyll *a* (μg g^{-1} wet), pheopigments (μg g^{-1} wet), abundance of *R. philippinarum* (g wet m^{-2}), and abundance of polychaete (g wet m^{-2}), respectively.

in overlying water under light conditions is evidence of the preference that microphytobenthos have for ammonium.

3.4.4 Nitrogen cycling in summer

Assuming that the difference in the nitrogen flux between light and dark conditions is explained by algal uptake processes, then the uptake rate of ammonium, nitrite, and nitrate from the overlying water can be calculated by subtracting the sediment-water flux under dark conditions from the sediment-water flux under light conditions. During September 1997, the algal uptake rate of ammonium, nitrite, and nitrate was calculated to be 125.1, 2.6, and 48.2 μmol N m^{-2} h^{-1}, respectively

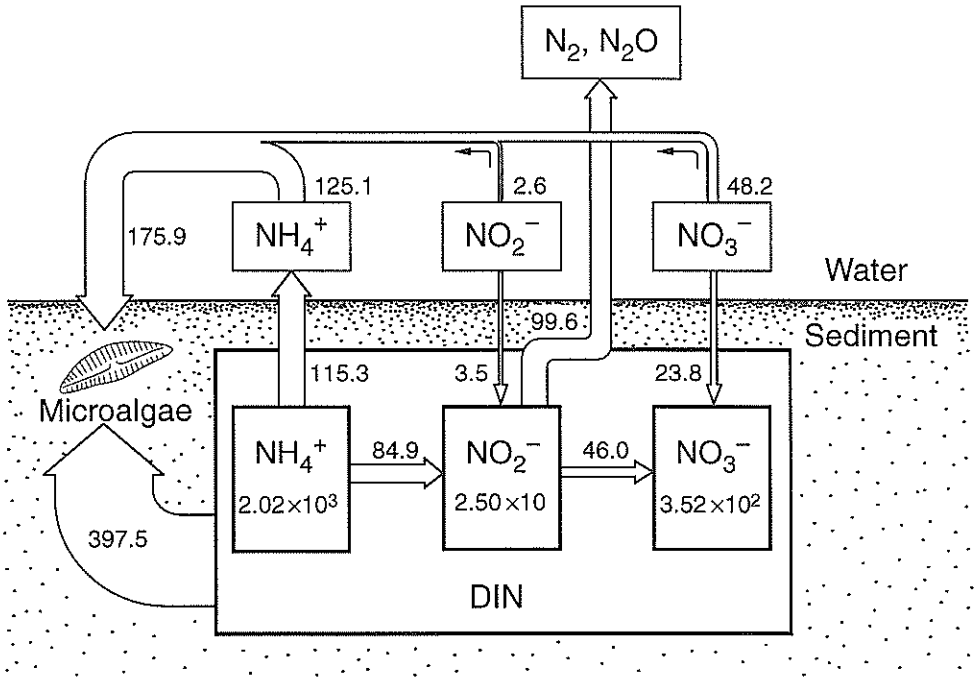

Figure 14 Dissolved inorganic nitrogen cycling during submerged and lightened period in September 1997. Values are for a depth of 5 cm on a m^2 basis. Fluxes are in μmol N m^{-2} h^{-1}. Standing stocks are in μmol N m^{-2}.

(**Figure 14**). It is likely that these rates are underestimates due to the possible uptake of nitrogen by benthic microalgae in the dark, which has been observed in several phytoplankton species (Malone et al., 1975). Therefore, my estimated uptake rate for nitrogen by microalgae from the overlying water may represent a minimum. The gross algal uptake of nitrogen estimated from oxygen productivity and the Redfield ratio is 573.4 μmol N m^{-2} h^{-1}, and consequently, at least 31% (175.9 μmol N m^{-2} h^{-1}) of the total algal uptake of nitrogen is derived from the overlying water, and the remainder (397.5 μmol N m^{-2} h^{-1}) from the porewater.

On a diurnal basis, the submerged and lightened time was 6 h on the sampling day, and during this period, benthic microalgae would use nitrogen directly from the water column (see section 3.4.3), accounting for 1.1 mmol N m^{-2} d^{-1}. The efflux of nitrogen during the submerged period (12 h) is calculated to be 1.1 mmol N m^{-2} d^{-1}, which is balanced with the algal uptake rate of nitrogen from the overlying water in the submerged and lightened period. This result indicates that microalgae on the sediment surface play a significant role in suppressing the release of mineralized nitrogen from the sediments into the overlying water.

3.4.5 Major contributor to denitrification

Denitrifying bacteria utilize nitrate as the terminal electron acceptor for the respiratory process (Nishio et al., 1982). The ambient nitrate concentration is widely reported as being the parameter most closely related to denitrification (e.g. Ogilvie et al., 1997; Christensen et al., 2000b). In the denitrification experiment, the concentration of nitrate in the overlying water was slightly higher than the mean nitrate concentration in the top 5 cm of the in situ sediment. Therefore, there is a possibility that the denitrification rate was overestimated. The measured denitrification rate was comparable to those found for samples from the other sandflat of Tokyo Bay (Sayama, 2000) and approximately six times higher than the maximum rate found in the shallow muddy sediments of the innermost part of Tokyo Bay (Sayama, 2001).

The Banzu intertidal sediment acted as a sink for nitrate in the present study (**Figure 12**), with consumption of nitrate greater than production. However, the rate of ammonium oxidation, which results in the production of nitrate, was comparable to that of denitrification, a nitrate consumption process. This suggests that another substantial nitrate consuming process, perhaps dissimilatory ammonium production, is present in the sediment.

This hypothesis is supported by the Eh profile, which was anaerobic in summer (**Table 4**). Denitrifiers and ammonifiers in sediments compete for nitrate, and the contribution of denitrification to total nitrate reduction has been reported to be 93% in Marlborough Sounds, New Zealand (Kasper et al., 1985), and 27 to 57% in the Tama estuary, Tokyo Bay (Nishio et al., 1982).

A strong coupling of nitrification and denitrification has been observed for several estuarine sediments (e.g. Jenkins and Kemp, 1984; Rysgaad et al., 1995; Ogilvie et al., 1997; Ottosen et al., 2001). Compared to nitrate derived from the overlying water, nitrate produced by nitrification can be a major contributor to sedimentary denitrification. In this study, even if the entire nitrate supplied from the water column is used for denitrification, this nitrate accounts for only 27% of total denitrification. This suggests that the major contributor to denitrification is sedimentary nitrate rather than nitrate derived from the overlying water (**Figure 14**). Therefore, the most important process in removing nitrogen from the overlying water in the Banzu intertidal flat is a coupled nitrification-denitrification process in sediments via degradation of organic nitrogen into ammonium rather than direct removal of nitrate by denitrification.

3.5 Conclusions

Intertidal sandflats are nutrient sinks, except during dark conditions in summer. Microalgae and, to some extent, bacteria on the sediment surface play a significant role in removing nutrients from the overlying water by assimilation and in suppressing the release of mineralized nutrients from the sediment. During dark conditions in summer, the intertidal sediment acts as a source of nutrients. Excretion of nutrients by the bivalve *Ruditapes philippinarum*, which dominates macrofauna at the site, greatly contributes to the net ammonium release flux at the sediment-water interface both spatially and temporally. Denitrification is also important in eliminating nitrate from the intertidal flat ecosystem. Denitrifiers preferentially utilize nitrate derived from the sediment more than from the overlying water.

3.6 Summary

Nitrification, denitrification, sediment-water nutrient exchange, and sedimentary oxygen production were simultaneously measured in the Banzu intertidal sandflat, Tokyo Bay, Japan. The sediment acted as a sink for both nitrate and phosphate under both light and dark conditions. The mean uptake rate of nitrate by the sediment was higher in the light (–65.3 μmol N m^{-2} h^{-1}) than in the dark (–34.6 μmol N m^{-2} h^{-1}) throughout the studied period. Most of the ammonium exchange fluxes in the light were also resulted in decreased ammonium in the overlying water. The mean uptake rate of ammonium by the sediment was markedly higher in the light (–41.1 μmol N m^{-2} h^{-1}) than in the dark (42.5 μmol N m^{-2} h^{-1}) throughout the studied period. These results indicate that microalgae and, to some extent, bacteria on the sediment surface play a significant role in removing nutrients from the overlying water by assimilation and in suppressing the release of mineralized nutrients from the sediment. During dark conditions in summer, the intertidal sediment acted as a source of ammonium. Excretion of nutrients by the bivalve *Ruditapes philippinarum*, which dominates macrofauna at the site, greatly contributed to the net release fluxes of ammonium at the sediment-water interface. In the summer of 1997, the total microphytobenthic uptake of nitrogen (nitrate + nitrite + ammonium) estimated from oxygen productivity and the Redfield ratio was 573.4 ± 64.4 μmol N m^{-2} h^{-1}, 31% of which was assumed to be derived from the overlying water. The release rate of nitrogen from the sediment to the water column (1.1 mmol N m^{-2} d^{-1}) was balanced with the removal rate of nitrogen from the water column by benthic microalgae on a diurnal basis. The measured denitrification rate using an acetylene inhibition technique was 99.6 ± 23.5 μmol N m^{-2} h^{-1} in summer. Since the direct supply of nitrate from the water column only accounted for 27% of the total denitrification at the highest estimate, nitrate in the sediment pool was the major contributor to sedimentary denitrification.

4. Role of Emersion and Inundation in the Porewater Nutrient Dynamics of Intertidal Sandflats

4.1 Introduction

Semi-diurnal movement of tidal water alters biotic and abiotic environments in intertidal sediments over short time intervals (Alongi, 1998). When sediments are exposed to air, the water table drops due to drainage and evaporation (Anderson and Howell, 1984; Agosta, 1985; Howes and Goehringer, 1994). At tidal flooding, in turn, vertical infiltration of tidal water controls interstitial water levels (Hemond and Fifield, 1982). Rhythmic emersion and immersion can also mediate the belowground transport of nutrients and metabolic products (Harvey and Odum, 1990; Dolphin et al., 1995). The role of advective solute transport in the distribution of nutrients has mainly been reported for salt marsh creekbanks (e.g. Agosta, 1985; Yelverton and Hackney, 1986; Nuttle, 1988; Howes and Goehringer, 1994) and sandy beaches (McLachlan and Illenberger, 1986; Uchiyama et al., 2000). In contrast, the movement of water and solutes associated with a fall in the water table has been reported to be minor in non-vegetative intertidal flats due to the development of a capillary fringe (Drabsch et al., 1999).

The biogeochemistry of intertidal sediments during immersion has been well studied in relation to the sed-

iment-water column exchange of nutrients (e.g. Falcão and Vale, 1990; Middelburg et al., 1995; Asmus et al., 1998; Falcão and Vale, 1998; Kuwae et al., 1998; Mortimer et al., 1999; Cabrita and Brotas, 2000; Magni et al., 2000). However, little is yet known of the dynamics of porewater nutrients in such sediments during emersion or transitional periods (Kerner et al., 1990; Rocha, 1998; Rocha and Cabral, 1998; Usui et al., 1998). During emersion, the penetration of oxygen into sediments may increase (Brotas et al., 1990), causing changes in the redox environment (Koch et al., 1992). This oxygenation affects the rates and pathways of nutrient flow (Kerner, 1993) related to, e.g., aerobic nitrifiers and anaerobic denitrifiers (Henriksen and Kemp, 1988; Seitzinger, 1988; Parkin, 1990). In addition, the absence of overlying waters indicates no efflux of nutrients from the sediment, which will either accumulate or be consumed within the sediments. Rocha (1998) has shown that total (dissolved and exchangeable) sedimentary ammonium accumulated during emersion. Usui et al. (1998) have reported that porewater nitrate decreased remarkably during the initial 3 to 4 hours after the onset of exposure. On the other hand, at tidal flooding, mixing of porewater with overlying water can result in drastic changes in the nutrient pool (Rocha, 1998; Rocha and Cabral, 1998). Rocha and Cabral (1998) have shown that approximately 80% of the nitrate pool was flushed at inundation.

This chapter reports the dynamics of porewater nutrients induced by tidal cycles in a eutrophic intertidal sandflat of Tokyo Bay, Japan. To my knowledge, this is the first report dealing with tide-induced temporal changes in the concentrations of three porewater nutrient species (nitrate, ammonium, and phosphate) during different seasons. Special emphasis is placed on (1) the influence of diffusive fluxes and advective transport on the pool size of nutrients during emersion and inundation; and (2) the role of emersion in microbial processes, including nitrification and nitrate reduction.

4.2 Materials and Methods

4.2.1 Study site

The sampling site is the same location as that in **Chapter 3** (the Banzu intertidal sandflat, see **Figure 8**). Details of the study area are shown in Section 3.2.1.

I conducted four seasonal surveys on the spring tide: March 1998, May 1998, September 1998, and November 1998. The tidal range on the survey days ranged from 1.1 to 1.6 m. No rainfall was recorded during surveys of the tidal flat.

4.2.2 Hydrology

To track fluctuations in the water table depth, a small well was dug into the sediment a few days before each survey. A polyvinyl chloride pipe (4.5-cm internal diameter), with holes drilled and covered with a nylon mesh, was placed in the well to a depth of 25 cm. Water levels in the pipe were measured using a float.

The diffusive efflux of nutrients from the sediment during immersion was calculated according to Fick's first law described by Berner (1980) as described in Section 3.2.3.

4.2.3 Sediment characteristics

At each survey, PAR, sediment temperature, Eh, porosity, water content, and chlorophyll *a* were measured. PAR was continuously measured during each sampling time using a Biospherical quantum sensor. Sediment temperature and Eh were measured in situ at intervals of 2 to 5 cm during emersion using a temperature probe (RT-10; Tabai Espec) and a platinum redox electrode (HM-14P; TOA). For the measurement of porosity and water content, core samples were taken to a depth of 1 cm with acrylic tubes (4.5-cm internal diameter) during both emersion (ca. 1 h before inundation) and immersion (ca. 1 h after inundation). Porosity and water content were determined by the weight loss after drying wet sediments at 90°C for 24 h. The remainder of each emersion-period core sample was used for the analysis of chlorophyll *a* in the sediment, extracted using 90% acetone solution, spectrophotometrically analyzed (U-3200; Hitachi) according to Lorenzen (1967).

4.2.4 Porewater solutes

On each survey day, sediment samples were taken every one to several hours from the onset of exposure to after submergence. Sediment cores ($n = 3$) were collected randomly from the site (2 m × 2 m) at each sampling, using an acrylic corer (8.6-cm internal diameter × 25-cm long). Sediment cores were immediately cut in situ into 2.5 to 10 mm segments, and sliced sediments were immediately fixed by dried ice in order to stop biogeochemical reactions. Fixed sediments were thawed and filled in syringes (10 ml) and were centrifuged for 10 min at 2,000 rpm (580 × *g*) at ambient temperature. Extracted water was filtered through a Millipore HA filter. Filtered water was immediately frozen for the later analysis of ammonium, nitrate, nitrite, and phosphate on an analyzer (TRAACS-800; Bran+Luebbe) and for the determination of salinity using a conductivity electrode (9382-10D; Horiba).

4.2.5 Statistical analysis

Linear regression was used to calculate the rate of change in porewater nutrient concentrations over the whole period of emersion. A one-way ANOVA was used to examine statistical differences in porewater nutrient concentrations between the last samples collected before inundation and the first samples collected after

Table 13 Characteristics of tide and porewater hydrology

	LWL[a] (cm)	HWL[a] (cm)	Emersed time (hour)	Lowest water table depth (cm)
Mar 98	–55	55–56	6.3	2.7
May 98	–97	57–60	8.2	5.1
Sep 98	–52	85–92	5.6	7.8
Nov 98	–31	85–89	4.9	3.4

[a]LWL, and HWL, low water level and high water level, respectively. Heights were from the sampling site.

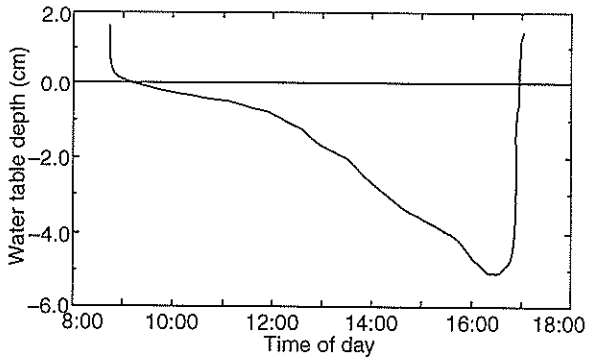

Figure 15 Representative data (May 1998) for the fall and rise of water table depth (cm) measured by using a small well during tidal exposure

inundation. Data sets were tested for homogeneity of variances (Hartley test), and the log-transformed values were used if needed for a normal distribution.

4.3 Results

4.3.1 Water table dynamics

The sediment water table measured by using a well dropped gradually following tidal exposure (**Figure 15**). Slightly before the onset of the next immersion, the water table dropped to its lowest level, and then rose steeply. This pattern was observed for all cases (not shown). The greatest water table drop (7.8 cm) occurred in summer (September 1998), and the smallest (2.7 cm) in winter (March 1998) (**Table 13**).

4.3.2 Sediment characteristics

The sampling days of March 1998 and May 1998 were cloudy, showing low PAR averages during the sampling time (108 to 152 μmol m^{-2} s^{-1}); the remainder showed high PAR values (499 to 639 μmol m^{-2} s^{-1}) (**Table 14**). During emersion, Eh was >0 mV for all seasons and depths, except below 5 cm in summer, when the mean sediment temperature in the top 10 cm reached a maximum (30.1°C) (**Figure 16**). Although there was a measurable decline in the water table level during emersion, no statistical differences in the water content and porosity were observed between emersion and immersion for any season ($P > 0.05$) (**Table 14**). Within the samples studied, the porosity and water content ranged from 44.6 ± 0.4 to 47.7 ± 1.0% (mean ± SE) and 23.6 ± 0.3 to 25.9 ± 0.8% (mean ± SE), respectively. Salinity of the porewater was close to that of tide water. The porewater never varied more than 3 psu from the tide water during the study. This strongly suggests that there was no significant ground water input. The chlorophyll *a* content in the top 10 mm of sediments ranged from 1.15 ± 0.16 to 8.33 ± 0.68 μg cm^{-3} (mean ± SE) (**Table 14**).

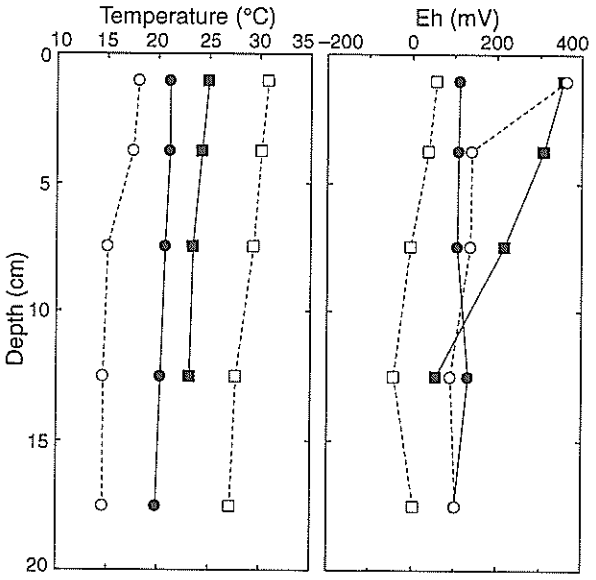

Figure 16 Vertical profiles of sedimentary temperature (°C) and redox potential (mV) during tidal exposure. Seasons: March 1998 (○); May 1998 (●); September 1998 (□); and November 1998 (■).

4.3.3 Porewater nutrient profiles

Depth profiles of porewater nitrate + nitrite (hereafter, nitrate) and phosphate during emersion showed marked concentration gradients with depth (**Figure 17**); nitrate and phosphate concentrations peaked in the uppermost layer of sediments for all the seasons, and below this they sharply declined until a depth of 30 mm. Nitrate concentrations in the upper layer peaked in November 1998 and were minimal in September 1998. Ammonium profiles either exhibited a stable pattern, or a gradual decrease in concentration from the sediment-

Table 14 Sediment water content and porosity during emersion (Em) and immersion (Imm), sediment chlorophyll *a* content, and photosynthetically available radiation (PAR) during sampling time

	Water content (%)[a]		Porosity (%)[a]		Chlorophyll *a*[a] (μg cm^{-3})	PAR (μmol m^{-2} s^{-1})
	Em[b]	Imm[c]	Em	Imm		
Mar 98	25.9 ± 0.8	24.7 ± 0.4	47.7 ± 1.0	46.1 ± 0.5	1.15 ± 0.16	108
May 98	24.8 ± 0.2	24.4 ± 0.4	46.2 ± 0.3	45.7 ± 0.5	4.49 ± 1.08	152
Sep 98	23.7 ± 0.3	24.1 ± 0.4	44.7 ± 0.4	45.2 ± 0.6	5.68 ± 0.41	639
Nov 98	24.6 ± 0.2	23.6 ± 0.3	46.1 ± 0.3	44.6 ± 0.4	8.33 ± 0.68	499

[a]Measured by using 0–10 mm depth sediments and are given as mean ± SE (n = 3).
[b]Samples were taken ca. 1 h before inundation.
[c]Samples were taken ca. 1 h after inundation.

water interface. All the nutrient concentrations in the uppermost sediments, except for nitrate in September 1998, were always higher than those in overlying waters.

4.3.4 Nutrient dynamics during emersion

Remarkable changes in nitrate and phosphate concentrations in the upper layers were observed during exposure, whereas deeper layers (>10 mm) showed only slight changes (**Figure 17**). A linear regression analysis revealed that the rates of change in nitrate concentration during emersion were statistically significant ($P < 0.05$) for most samples of the top 10 mm sediments, ranging from –6.6 to 4.8 μmol N liter^{-1} bulk sed. h^{-1} (**Figure 18**). However, these rates approached zero below 20 mm depth. Ammonium concentration decreased with time, except for the summer samples (**Figure 17**). The rates of change in ammonium concentration were near constant with depth, in contrast to the rates measured for other nutrient species (**Figure 18**). The maximum rate of decrease in ammonium concentration (–22.9 μmol N liter^{-1} bulk sed. h^{-1}) was observed in the deeper layer (20 to 25 mm) in spring, whereas the maximum rate of increase (11.8 μmol N liter^{-1} bulk sed. h^{-1}) was observed in the deepest layer (90 to 100 mm) in summer (not shown). Few statistically significant rates of change in phosphate concentration were measured (**Figure 18**); the greater changes were observed in the upper layers than in the deeper layers (>30 mm).

4.3.5 Nutrient dynamics at inundation

Nitrate and phosphate concentrations in the top layers showed marked changes at tidal flooding as well as during exposure (**Figure 17**). The concentrations of nitrate and phosphate in the top 10 mm layers declined at inundation for most of all seasons (**Figure 19**). These declines resulted in loss of the nitrate pool (–4 to 68%, mean: 32.8%) and the phosphate pool (–4 to 44%, mean: 20.8%) in the top 10 mm of sediments. The patterns of change in ammonium concentration were constant with depth except for those measured in May 1998 (**Figure 19**).

4.4 Discussion

4.4.1 Porewater hydrology

The water content of the Banzu intertidal surface sediment did not change significantly following tidal exposure although measurable movement was found for the water table depth (where pore pressure equals atmospheric pressure) (**Figure 15**). This could be attributed to the development of a capillary fringe above the water table depth (where pore pressure is less than atmospheric pressure) and a high moisture retention capacity at the top of the sandy sediments (Drabsch et al., 1999). Hence, interstitial water and solutes were probably held at the surface during emersion and little transport occurred into deeper sediments. Drabsch et al. (1999) found that the water table fell only a few centimeters below the sediment surface of an intertidal sandflat in Manukau Harbour, New Zealand, and the top of the sediments remained close to saturation throughout the tidal cycle. Hemond and Fifield (1982) examined the hydrological regime in a peaty, New England marsh and found seepage rates to be low, and also found that sediments remained saturated throughout the tidal cycle. In contrast, emersion of intertidal areas resulted in surface sediment water contents decreasing by 3.5% at Tama estuary in Tokyo Bay (Usui et al., 1998), and by more than 10% in Sado estuary (Rocha, 1998). The main reason for the discrepancy in water content dynamics during emersion between sites is probably due to differences in the length of emersion time, topographical slope, and substrate type (permeability). It is also possible that

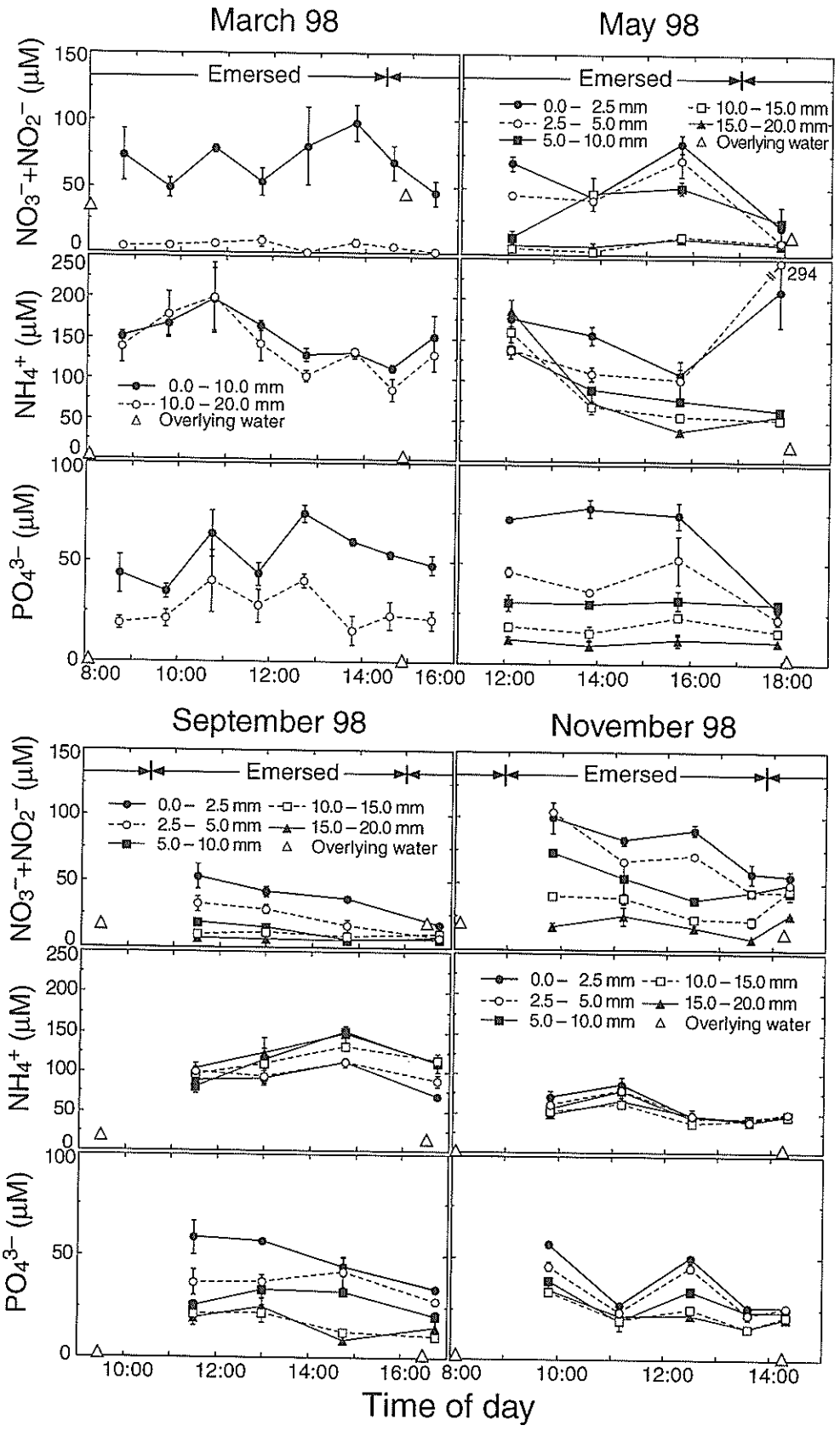

Figure 17 Temporal changes in interstitial nutrient concentrations (μM). Error bars indicate standard errors (n = 3). Only data from the top 20 mm sediment are shown to improve clarity. Note that the depth interval for March 98 is different from the other seasons.

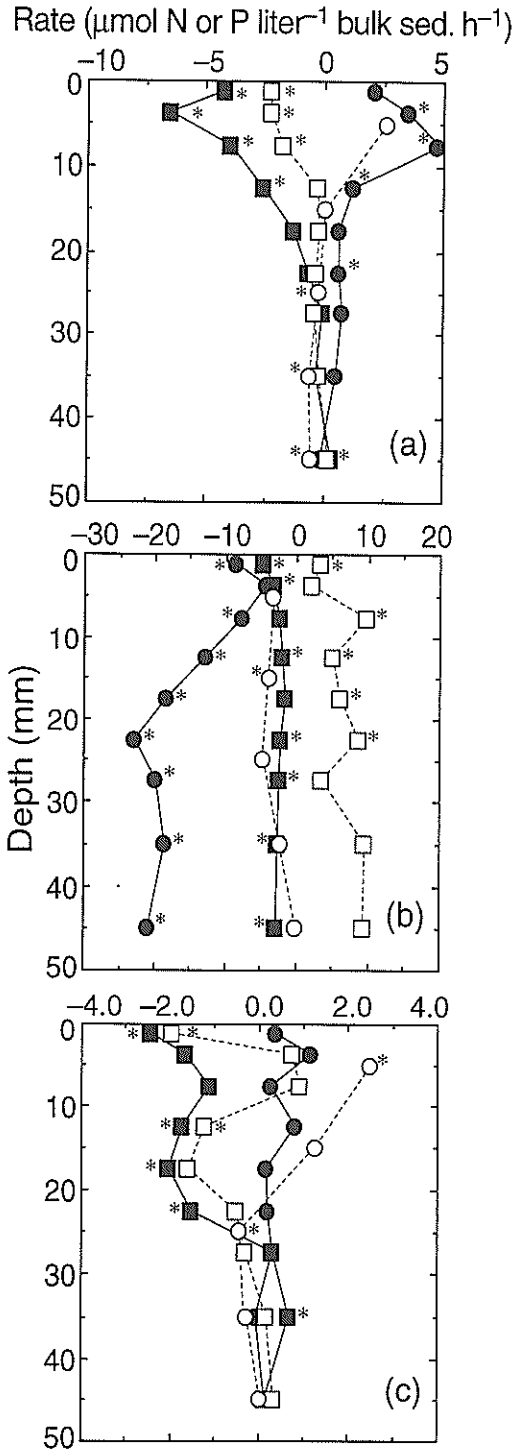

Figure 18 Rates of change in interstitial nitrate+nitrite (a), ammonium (b), and phosphate (c) concentrations (μmol N or P liter^{-1} bulk sed. h^{-1}) during the whole period of emersion. Seasons: March 1998 (○); May 1998 (●); September 1998 (□); and November 1998 (■). The rates were calculated using a linear regression analysis. Plots with asterisks indicate statistically significant rates of change at the 5% level.

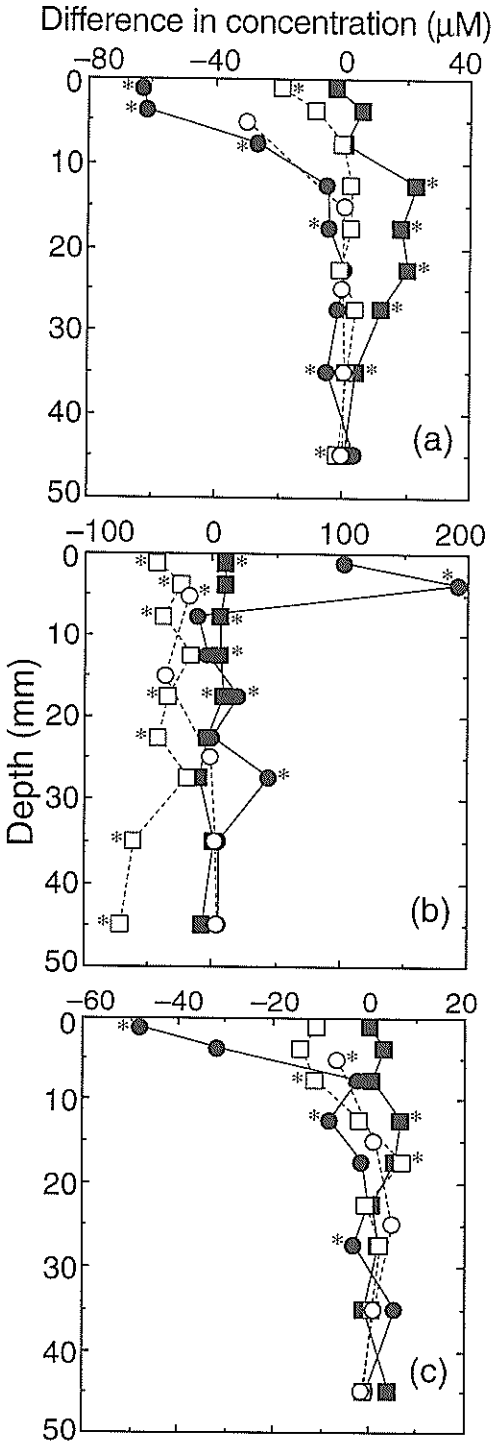

Figure 19 Differences in interstitial nitrate+nitrite (a), ammonium (b), and phosphate (c) concentrations (after inundation – before inundation) (μM). Seasons: March 1998 (○); May 1998 (●); September 1998 (□); and November 1998 (■). Plots with asterisks indicate statistically significant differences in concentration at the 5% level using a one-way ANOVA (n = 3).

Table 15 Observed rate of change in porewater nutrient concentration (Obs), diffusive flux contribution (Diff), and rate of nutrient production (Prod) during emersion

	Depth (mm)	$NO_3^- + NO_2^-$				NH_4^+				PO_4^{3-}			
		Obs[ab]	Diff[ac]	Prod[ad]	Diff/Obs (%)	Obs	Diff	Prod	Diff/Obs (%)	Obs	Diff	Prod	Diff/Obs (%)
Mar 98	0–10	2.6	–1.0	3.6	–37	–3.3	–0.2	–3.1	5	2.5	–0.1	2.6	–3
	10–40	–0.3	0.3	–0.6	–121	–4.0	0.0	–4.0	1	0.2	0.0	0.2	9
May 98	0–2.5	2.0	–3.5	5.5	–174	–8.7	–11.2	2.5	129	0.4	–2.0	2.4	–556
	2.5–5.0	3.5	1.3	2.2	36	–4.4	9.5	–13.9	–219	1.1	1.6	–0.5	138
	5.0–10	4.8	–0.5	5.3	–11	–7.8	0.9	–8.7	–11	0.3	0.0	0.3	3
	10–40	0.7	0.3	0.4	45	–18.6	0.0	–18.6	0	0.3	0.0	0.3	14
Sep 98	0–2.5	–2.3	–4.9	2.6	209	3.3	2.0	1.3	61	–2.0	–2.2	0.2	113
	2.5–5.0	–2.3	2.3	–4.6	–99	1.9	–1.8	3.7	–95	0.7	1.7	–1.0	228
	5.0–10	–1.8	0.8	–2.6	–46	9.7	0.3	9.4	3	0.9	0.1	0.8	8
	10–40	–0.4	0.1	–0.5	–26	6.4	0.0	6.4	0	–0.7	0.0	–0.7	–3
Nov 98	0–2.5	–4.4	–3.0	–1.4	68	–4.8	–1.6	–3.2	34	–2.5	–0.6	–1.9	23
	2.5–5.0	–6.6	–1.8	–4.8	27	–3.5	1.0	–4.5	–28	–1.7	0.1	–1.8	–6
	5.0–10	–4.0	0.9	–4.9	–23	–2.6	–0.3	–2.3	11	–1.1	0.1	–1.2	–11
	10–40	–1.0	0.3	–1.3	–27	–2.2	0.1	–2.3	–5	–0.9	0.0	–0.9	–1

[a]All values are in mmol N or P m^{-3} bulk sed. h^{-1}. All values for the 10–40 mm depth were averaged (Mar 98: $n = 3$; others: $n = 6$).

[b]Same data as **Figure 18**.

[c]Calculated using Fick's second law of diffusion. Negative values indicate loss of nutrients.

[d]Estimated as: Obs – Diff. Negative values of Prod indicate consumption of nutrients.

porewater around large macrobenthic burrows is more mobile (Allanson et al., 1992), and therefore independent of capillary fringe processes. This greater fluid channeling through burrows may influence nutrient dynamics. Nevertheless, during emersion, the influence of advection on porewater nutrient dynamics is minor at my site, which is characterized by short-emersion-time, low-slope, low-permeability, and no large-burrows.

4.4.2 Effect of diffusive fluxes during emersion

The porewater hydrology described above shows that all spatial transport of solutes in the sediment is assumed to have taken place by 1-demensional diffusion, i.e., both horizontal and vertical advection caused by hydraulic gradients or water table movement, can be neglected. Therefore, the transport process can be described by Fick's second law of diffusion (Berner, 1980). The relationship between diffusive transport and the rate of solute production can be described as follows (Rysgaard and Berg, 1996):

$$\varphi \frac{\partial C}{\partial t} = D_S \frac{\partial}{\partial x}\left[\varphi \frac{\partial C}{\partial x}\right] + P \qquad (3)$$

where φ is the porosity, C is the concentration of the nutrient species in the porewater, t is the time, D_S is the sediment diffusion coefficient, x is the depth, and P is the rate of production or consumption of the nutrient species per unit volume of sediment.

Table 15 shows that diffusive flux of all nutrient species during emersion contributed greatly to the observed rate of change in the porewater nutrient concentration of the surface sediment (0 to 10 mm). The influence of diffusive flux is less for the subsurface layer (10 to 40 mm). This reflects steeper nutrient concentration gradients in the near-surface compared to the deeper environment (**Figure 17**).

4.4.3 Effect of microbial processes during emersion

Nutrient production rates during emersion were estimated by subtracting diffusive flux from the observed rate of change in nutrient concentration (**Table 15**). The

range of the estimated production rates were: (1) nitrate: −4.9 to 5.5 mmol N m^{-3} bulk sed. h^{-1}; (2) ammonium: −18.6 to 9.4 mmol N m^{-3} bulk sed. h^{-1}; and (3) phosphate: −1.9 to 2.6 mmol P m^{-3} bulk sed. h^{-1}. Obviously, much higher nitrate concentrations in the surface sediment than in the overlying water (**Figure 17**) indicate a high nitrification activity in the Banzu intertidal flat sediment. Moreover, in situ nitrification rates are likely to be higher than the estimated nitrate production rates, which may include microbial nitrate reduction as well as nitrification. Nevertheless, in general, only the topmost layer showed nitrate production, being the main site of nitrification (Koike and Sørensen, 1988). Nitrate in the 2.5 to 10.0 mm sediment was supplied through molecular diffusion from the topmost layer (0 to 2.5 mm) and was largely consumed within this layer. This indicates that microbial nitrate reduction within the subsurface sediment, including denitrification and dissimilatory ammonification (Fenchel et al., 1998), is strongly supported by diffusive influx of nitrate from the surface sediment, where nitrification activity is high. Supply of high concentrations of nitrate into deeper layers during emersion may support some stocks of nitrate and the stimulation of deeper layer denitrification (Alongi et al., 1999). Alongi et al. (1999) speculated that the rapid denitrification rates measured for intertidal mudflat and mangrove forest sediments reflect a vertically expanded zone of denitrification caused by the presence of nitrate in deeper sediments.

In summer, the rate of ammonium production was stimulated for all of the sediment layers (**Table 15**); this coincided with the highest observed temperatures (**Figure 16**). Ammonium production processes probably include dissimilatory ammonium production and mineralization. Temperature dependence of benthic mineralization has been observed for various shallow environments (e.g. Jørgensen and Sørensen, 1985; Middelburg et al., 1996; Trimmer et al., 1998; Trimmer et al., 2000). In addition, low Eh within the deeper layers (**Figure 16**) is evidence of anaerobic decomposition of accumulated organic matter. Dissimilatory ammonium production in the deeper layers was probably only a minor contributor to total ammonium production due to low nitrate concentrations (**Figure 17**).

I plotted the production rates of nitrate and ammonium versus the emersion time of the sediment in order to investigate if emersion-related oxygenation influences production rates in the subsurface layer (2.5 to 10 mm) (**Figure 20**). The rate of nitrate production was stimulated in proportion to the emersion time (r = 0.80, P = 0.029), whereas the rate of ammonium production was inhibited (r = 0.51, P = 0.240). These relationships indicate a weakening of the anoxic environment by oxygenation during exposure, and subsequent (1) stimulation of nitrification; or (2) inhibition of nitrate reduction; or (3)

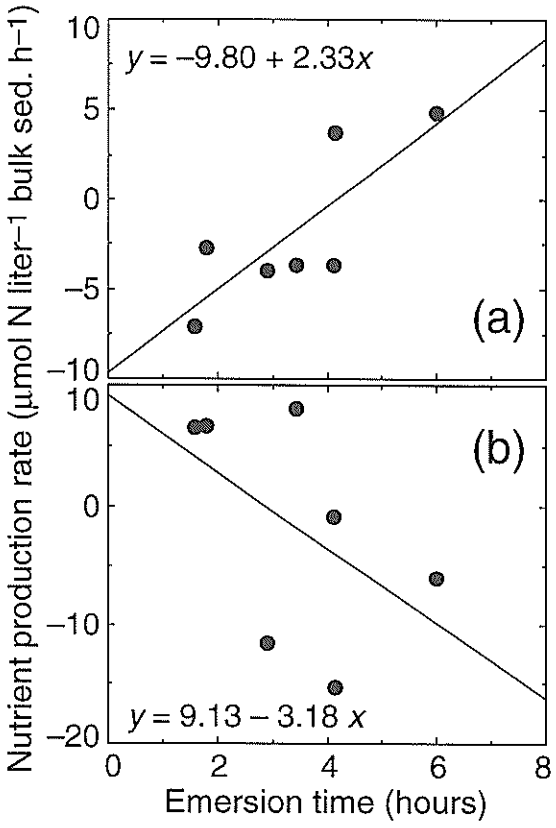

Figure 20 Volumetric nitrate (a) and ammonium (b) production rates (µmol N $liter^{-1}$ bulk sed. h^{-1}) (depth: 2.5–10 mm) versus emersion time. The production rates were calculated by subtracting molecular diffusive fluxes from the observed rates of change in concentration (see **Table 15**). Negative values indicate the consumption of nutrients.

a combination of both processes. With regard to this emersion-related oxygenation, Koch et al. (1992) found that Eh increased during exposure of mudflat subsurface sediments (3 to 5 mm) in River Torridge, England. My observed relationship between the rate of nitrate production and the emersion time is consistent with nitrate behavior in Tama estuary sediments, Japan, where the nitrate pool was constant or slightly increased 3 to 4 hours after the onset of exposure (Usui et al., 1998).

Understanding the other mechanisms affecting porewater nutrient concentration needs further investigation. For instance, porewater nutrients can be assimilated by microphytobenthos during emersion as well as during immersion because of their high levels of productivity at the site (see **Chapter 3**). The decrease in phosphate concentration on sunny days of September 1998 and November 1998 (**Table 14** and **Figure 18**) might support the active microalgal photosynthesis and the following uptake of phosphate from porewater during expo-

Table 16 Inventory of porewater nutrients (μmol N or P m^{-2}, depth: 0–10 mm) before (B) and after (A) inundation

		B	A	Diff(s)[a]	Diff(s)/A (%)	Diff(s–w)[b]	Diff(s–w)/A (%)	ΔI[c]
$NO_3^- + NO_2^-$	Mar 98	474	330	12	4	2	1	–130
	May 98	305	98	25	26	7	7	–175
	Sep 98	78	49	–1	–2	–2	–4	–32
	Nov 98	220	229	6	3	32	14	47
NH_4^+	Mar 98	626	538	0	0	6	1	–82
	May 98	415	730	13	2	237	32	565
	Sep 98	608	442	14	3	67	15	–85
	Nov 98	192	227	1	0	36	16	72
PO_4^{3-}	Mar 98	286	254	1	0	1	0	–30
	May 98	224	126	2	2	7	6	–89
	Sep 98	174	118	5	4	8	7	–43
	Nov 98	109	114	1	1	18	16	24

[a]Diff(s), mass transport of porewater nutrients within the sediments occurred by molecular diffusion. Values are estimated as: diffusive flux calculated by Fick's second law of diffusion × time, where time is measured between the last sampling before inundation and the first sampling after inundation. Positive values indicate effluxes to the deeper layers.

[b]Diff(s–w), mass transport of porewater nutrients across the sediment-water interface occurred by molecular diffusion. Values are estimated as: diffusive flux calculated by Fick's first law of diffusion × time, where time is measured between inundation and the first sampling after inundation. Positive values indicate nutrient release from the sediments.

[c]Estimated as: A – (B – Diff(s) – Diff(s–w)).

sure. Diurnal variation in nitrification and denitrification can also mediate the pool size of nutrients (Ottosen et al., 2001). Using a new ^{15}N-ammonium spray technique, Ottosen et al. (2001) demonstrated that coupled nitrification-denitrification rates during the day were lower than at night in exposed intertidal mudflats of the Tagus estuary. In addition, data on the fraction of nutrients adsorbed on the sediment particles can help to understand the dynamics of porewater ammonium and phosphate (Mesnage and Picot, 1995; Rocha, 1998; Slomp et al., 1998; Sundareshwar and Morris, 1999; Suzumura et al., 2000).

4.4.4 Nutrient dynamics at inundation

The concentration of interstitial nutrients changed markedly at tidal flooding, however, with the exception of the decrease in nitrate and phosphate in the surface layer, the concentration patterns were not simple (**Figure 19**). For instance, in the topmost sediment sampled in May 1998, the concentration of nitrate and phosphate decreased, but that of ammonium markedly increased. These complicated results relate partially to the low-time-resolution of the dynamics of each nutrient during the transitional tidal phase. Nevertheless, nitrate loss in surface sediments at inundation has also been reported by Rocha and Cabral (1998). They showed approximately 80% of the nitrate pool to be flushed at inundation of the Sado estuary. Similar results were reported for ammonium and phosphate (Rocha et al., 1995; Falcão and Vale, 1998; Rocha, 1998). Rocha et al. (1995) found that an abrupt rise in ammonium concentration occurred in the water column during the first hour of flood in the Sado estuary. Falcão and Vale (1998) showed that during 20 minutes of inundation, large quantities of ammonium and phosphate were transported to the overlying water in a coastal lagoon of Ria Formosa. Rocha (1998) reported that ~75% of total (dissolved and exchangeable) sedimentary ammonium was exported within 45 min of inundation.

Factors affecting solute dynamics at inundation and during immersion periods can include (1) infiltration; (2) molecular diffusion; (3) external forces caused by tidal currents and waves; (4) free convention; and (5) bioturbation. The effect of infiltration is possibly not large for my case, because water content in the sediment did not change according to tidal regime. I calculated mass transport of interstitial nutrients occurred by molecular diffusion within the sediments (Diff(s)) and across the

sediment-water interface (Diff(s–w)) (**Table 16**). The contribution of molecular diffusion to mass transport of nutrients after inundation in the top 10 mm sediments was minor for both Diff(s) (–2 to 26%, mean: 3.5%) and Diff(s–w) (–4 to 32%, mean: 9.2%). Therefore, the decrease in some interstitial nutrients in the surface layer can not be explained by molecular diffusion alone. The external forces caused by tidal currents and waves can account for mixing of porewater with overlying water. de Jonge and van Beusekom (1995) speculated that the surface layer is more permeable as a result of hydrodynamic reworking. Inoue and Nakamura (2000) have shown theoretically that an abrupt increase in shear velocity can lead to a drastic increase in the phosphate flux (1.7 times higher than steady state) at the sediment-water interface during the first 30 minutes of the experiment. They speculated that turbulent diffusion resulted in the rapid upward transport of accumulated phosphate within the concentration boundary layer. In addition, Inoue and Nakamura (2000) found that a steep oxygen concentration increase in overlying water resulted in a change in the direction as well as the rate of phosphate flux, due to enhancement of phosphate adsorption by the sediment. My complicated porewater nutrient dynamics at inundation may be partially explained by these externally controlled physico-chemical interactions. Free convection due to the temperature gradients within sediments, and between sediments and flooding water, can also promote mixing of porewater with overlying water (Webster et al., 1996; Rocha, 1998; Rocha and Cabral, 1998). Many workers have suggested that macrofaunal reworking can cause much higher nutrient fluxes than molecular diffusion (e.g. Kikuchi, 1986; Webster, 1992; Davey and Partridge, 1998; Mortimer et al., 1999; Christensen et al., 2000a; Hughes et al., 2000). Higher macrofaunal abundances at my site (**Table 5**), and associated enhanced bioturbation, would also increase nutrient efflux from the sediments.

All of the processes described above promote mixing of porewater with overlying water. Thus, in my case, mixing of low-nutrient overlying water (**Figure 17**) with nutrient-rich porewater results in porewater nutrient depletion by dilution. Therefore, the increase in porewater ammonium for May 1998 is attributed to other mechanisms. These may include ongoing microbial reactions after emersion, and other mechanisms, such as stimulation of macrofaunal excretion during sediment reworking.

4.5 Conclusions

The water content in the surface sediment of the Banzu intertidal sandflat does not change significantly although a measurable decline in water table depth during emersion is found. Consequently, it is concluded that the influence of advective transport caused by a fluctuating water table on porewater nutrient dynamics is minor for my site. During emersion, the diffusive flux of all nutrient species greatly contributes to the observed rate of change in porewater nutrient concentration for the surface sediment. Microbial nitrate reduction, including denitrification and dissimilatory ammonification, within the subsurface sediment is strongly fueled by downward diffusive flux of nitrate from the surface sediment. A promotion of nitrate production rate and decline of ammonium production rate proportional to the emersion time of the subsurface layer indicates a weakening of the anoxic environment by oxygenation during exposure, and subsequent stimulation of nitrification or inhibition of nitrate reduction. The marked decrease in interstitial nitrate and phosphate concentrations in the surface layer at inundation cannot be explained by molecular diffusion alone.

4.6 Summary

Porewater nutrient dynamics during emersion and at inundation were investigated during different seasons in a eutrophic intertidal sandflat of Tokyo Bay, Japan, to elucidate the role of emersion and inundation in solute transport and microbial processes. The water content in the surface sediment did not change significantly following tidal exposure, suggesting that advective solute transport caused by water table fluctuation was negligible for the Banzu intertidal sandflat. The rate of change in nitrate concentration in the top 10 mm of sediments ranged from –6.6 to 4.8 μmol N liter^{-1} bulk sed. h^{-1} during the whole period of emersion. Steep nutrient concentration gradients in the surface sediment generated diffusive flux of nutrients directed downwards into deeper sediments, which greatly contributed to the observed rate of change in porewater nutrient concentration. Microbial nitrate reduction within the subsurface sediment, including denitrification and dissimilatory ammonification, was strongly supported by the downward diffusive flux of nitrate from the surface sediment. The stimulation of nitrate production rate in the subsurface layer in proportion to the emersion time indicates that oxygenation due to emersion caused changes in the sediment redox environment and affected both the nitrification and nitrate reduction rates. The nitrate and phosphate pools in the top 10 mm of sediments decreased markedly at tidal flooding (up to 68% for nitrate and up to 44% for phosphate), however, this result could not be solely explained by molecular diffusion.

5. Conclusions

The present study aimed to elucidate the biogeochemical role of benthic microorganisms in intertidal sandy sediments. The following results were obtained.

(1) I measured the abundance and biovolume of bacteria in intertidal sediments from Tokyo Bay, Japan, by using a dual-staining technique (4′,6-diamidino-2-phenylindole and acridine orange) and several dispersion techniques (ultrasonic cleaner, ultrasonic sonicator, and tissue homogenizer). Dual staining reduced the effect of background fluorescence, particularly when used for silt-, clay-, and detritus-rich sediments, and allowed us to distinguish bacteria from other objects during measurement of both bacterial cell abundance and size. Within the studied samples, the number of bacterial cells ranged from 0.20×10^9 to 3.54×10^9 g of wet sediment^{-1}. Applying the ultrasonic cleaner and sonicator treatments to disperse bacteria, the numbers of bacteria for all of the sites initially increased with dispersion time and then became constant. After applying the homogenizer treatments, the highest cell numbers were observed for the shortest treatment times (0.5- to 2-min), and bacterial cell counts then declined steeply as the homogenization time increased, indicating that cell destruction occurred. Application of the ultrasonic cleaner treatment sometimes caused insufficient dispersion of bacteria for fine-grain sediments. Within the studied samples, the bacterial biovolume ranged from 0.07 to 0.22 μm^3. Applying the ultrasonic cleaner and sonicator treatments, the biovolume peaked during shorter dispersion times. This pattern was caused not by cell destruction but by the incremental portion of dispersed small cells. I concluded that application of the ultrasonic cleaner and sonicator treatments over longer dispersion times reflected the real bacterial cell size spectrum and was preferable for accurate estimation of mean bacterial biovolumes. The findings described above can contribute to a better understanding of the role of bacterial biomass in immobilized nutrient pools and associated rates of nutrient flux; however, further investigations are required for a quantitative estimation of the role of immobilized nutrient pools in nutrient cycling.

(2) Nitrification, denitrification, sediment-water exchange, and oxygen production were simultaneously measured for two years in the Banzu intertidal sandflat, Tokyo Bay, Japan. The sediment acted as a sink for both nitrate and phosphate under both light and dark conditions. The mean uptake rate of nitrate by the sediment was higher in the light (–65.3 μmol N m^{-2} h^{-1}) than in the dark (–34.6 μmol N m^{-2} h^{-1}) throughout the studied period. The sediment also mainly acted as a sink for ammonium in the light. The mean uptake rate of ammonium by the sediment was markedly higher in the light (–41.1 μmol N m^{-2} h^{-1}) than in the dark (42.5 μmol N m^{-2} h^{-1}) throughout the studied period. These results indicate that microalgae and, to some extent, bacteria on the sediment surface play a significant role in removing nutrients from the overlying water by assimilation and in suppressing the release of mineralized nutrients from the sediment. During dark conditions in summer, the intertidal sediment acted as a source of ammonium. Excretion of nutrients by the bivalve *Ruditapes philippinarum*, which dominates macrofauna at the site, greatly contributed to the net release fluxes of ammonium at the sediment-water interface. In the summer of 1997, the total microphytobenthic uptake of nitrogen (nitrate + nitrite + ammonium) estimated from oxygen productivity and the Redfield ratio was 573.4 ± 64.4 μmol N m^{-2} h^{-1}, 31% (175.9 ± 64.4 μmol N m^{-2} h^{-1}) of which was assumed to be derived from the overlying water. The release rate of nitrogen from the sediment to the water column (1.1 mmol N m^{-2} d^{-1}) was balanced with the removal rate of nitrogen from the water column by benthic microalgae on a diurnal basis. The measured denitrification rate using an acetylene inhibition technique was 99.6 ± 23.5 μmol N m^{-2} h^{-1} in summer. Since the direct supply of nitrate from the water column only accounted for 27% of the total denitrification at the highest estimate, nitrate in the sediment pool was the major contributor to sedimentary denitrification.

(3) Porewater nutrient dynamics during emersion and at inundation were investigated during different seasons in a eutrophic intertidal sandflat of Tokyo Bay, Japan, to elucidate the role of emersion and inundation in solute transport and microbial processes. The water content in the surface sediment did not change significantly following tidal exposure, suggesting that the advective solute transport caused by water table fluctuation was negligible for the Banzu intertidal sandflat, which is characterized by short-emersion-time and low-slope. The rate of change in nitrate concentration in the top 10 mm of sediments ranged from –6.6 to 4.8 μmol N liter^{-1} bulk sed. h^{-1} during the whole period of emersion. Steep nutrient concentration gradients in the surface sediment generated diffusive flux of nutrients directed downwards, which contributed greatly to the observed rate of changes in the porewater nutrient concentration. Microbial nitrate reduction within the subsurface sediment, including denitrification and dissimilatory ammonification, was strongly supported by the downward diffusive flux of nitrate from the surface sediment. The stimulation of nitrate production rate in the subsurface layer in proportion to the emersion time indicates that oxygenation due to emersion caused changes in the sediment redox environment and affected both the nitrification and nitrate reduction rates. The nitrate and phosphate pools in the top 10 mm of sediments decreased markedly at tidal flooding (up to 68% for nitrate and up to 44% for phosphate), however, this result could not be solely explained by molecular diffusion.

(Received on November 30, 2001)

Acknowledgments

I would like to thank my present and former bosses, Dr. Hiroaki Ozasa, Dr. Yasushi Hosokawa, Dr. Yoshiyuki Nakamura, Mr. Eiichi Miyoshi, Mr. Keita Furukawa, and Mr. Takeshi Suzuki of the Port and Airport Research Institute, for giving me the opportunity to research intertidal flat biogeochemistry and ecology and for their helpful suggestions and in-depth discussion of my work.

I would also like to express my sincere gratitude to my present and former colleagues, including Mr. Eiji Kibe, Mrs. Naoko Kobayashi, Dr. Munehiro Nomura, Mr. Yukimasa Hagimoto, and Dr. Susumu Konuma of the Coastal Ecosystems Division, Port and Airport Research Institute, for their kind help during fieldwork and analytical work, and for their encouragement.

Appreciation is especially extended to Professor, Dr. Hiroyuki Nakahara, the Division of Applied Biosciences, Graduate School of Agriculture, Kyoto University for his supervision and guidance, and for the many valuable suggestions he made on the present study.

I would also like to express gratitude to Professors, Drs. Aritsune Uchida and Wataru Sakamoto of the Graduate School of Agriculture, Kyoto University for their valuable comments on my work. Special thanks go to Associate Professors, Drs. Ichiro Imai and Tateki Fujiwara of the Graduate School of Agriculture, Kyoto University for their valuable input into my professionalism as a researcher.

The present study was supported in part by a grant from the former Environment Agency of Japan.

References

Agosta, K. (1985): The effect of tidally induced changes in the creekbank water table on pore water chemistry. *Estuar. Coast. Shelf Sci.* **21**:389–400.

Allanson, B. R., Skinner, D., and Imberger, J. (1992): Flow in prawn burrows. *Estuar. Coast. Shelf Sci.* **35**: 253–266.

Alongi, D. M. (1988): Bacterial productivity and microbial biomass in tropical mangrove sediments. *Microb. Ecol.* **15**:59–79.

Alongi, D. M. (1991): The role of intertidal mudbanks in the diagenesis and export of dissolved and particulate materials from the Fly Delta, Papua New Guinea. *J. Exp. Biol. Ecol.* **149**:81–107.

Alongi, D. M. (1998): Coastal ecosystem processes. CRC Press, Boca Raton, Florida.

Alongi, D. M., Tirendi, F., Dixon, P., Trott, L. A., and Brunskill, G. J. (1999): Mineralization of organic matter in intertidal sediments of a tropical semi-enclosed delta. *Estuar. Coast. Shelf Sci.* **48**:451–467.

Anderson, F. E., and Howell, B. A. (1984): Dewatering of an unvegetated muddy tidal flat during exposure — desiccation or drainage? *Estuaries* **7**:225–232.

Aoyama, H., and Suzuki, T. (1996): The quantitative evaluation about water purification function on tidal flat in Mikawa Bay. *Report AFRI* **3**:17–28 (in Japanese).

Asmus, R. M., Jensen, M. H., Jensen, K. M., Kristensen, E., Asmus, H., and Wille, A. (1998): The role of water movement and spatial scaling for measurement of dissolved inorganic nitrogen fluxes in intertidal sediments. *Estuar. Coast. Shelf Sci.* **46**:221–232.

Balderston, W. L., Sherr, B., and Payne, W. J. (1976): Blockage by acetylene of nitrous oxide reduction in *Pseudomonas perferctomarinus*. *Appl. Environ. Microbiol.* **31**:504–508.

Berner, R. A. (1980): Early diagenesis: a theoretical approach. Princeton University Press, Princeton.

Bianchi, M., Bonin, P., and Filiatra, M. (1994): Bacterial nitrification and denitrification rates in the Rhône river plume (northwestern Mediterranean Sea). *Mar. Ecol. Prog. Ser.* **103**:197–202.

Blackburn, T. H., and Henriksen, K. (1983): Nitrogen cycling in different types of sediments from Danish waters. *Limnol. Oceanogr.* **28**:477–493.

Blackburn, T. H. (1986): Nitrogen cycle in marine sediments. *Ophelia* **26**:65–76.

Blackburn, N., Hagström, Å., Wikner, J., Cuadros-Hansson, R., and Bjørnsen, P. K. (1998): Rapid determination of bacterial abundance, biovolume, morphology, and growth by neural network-based image analysis. *Appl. Environ. Microbiol.* **64**:3246–3255.

Bloem, J., Veninga, M., and Shepherd, J. (1995): Fully automatic determination of soil bacterium numbers, cell volumes, and frequencies of dividing cells by confocal laser scanning microscopy and image analysis. *Appl. Environ. Microbiol.* **61**:926–936.

Bodelier, P. L., Libochant, J. A., Blom, C. W. P. M., and Laanbroek, H. J. (1996): Dynamics of nitrification and denitrification in root-oxygenated sediments and adaptation of ammonia-oxidizing bacteria to low-oxygen or anoxic habitats. *Appl. Environ. Microbiol.* **62**:4100–4107.

Bolalek, J., and Graca, B. (1996): Ammonia nitrogen at the water-sediment interface in Puck Bay (Baltic Sea). *Estuar. Coast. Shelf Sci.* **43**:767–779.

Brotas, V., Amorim-Ferreira, A., Vale, C., and Catarino, F. (1990): Oxygen profiles in intertidal sediments of Ria Formosa (S. Portugal). *Hydrobiol.* **207**:123–129.

Cabrita, M. T., and Brotas, V. (2000): Seasonal variation in denitrification and dissolved nitrogen fluxes in intertidal sediments of the Tagus estuary, Portugal. *Mar. Ecol. Prog. Ser.* **202**:51–65.

Callender, E., and Hammond, D. E. (1982): Nutrient exchange across the sediment-water interface in the Potomac River Estuary. *Estuar. Coast. Shelf Sci.* **15**: 395–413.

Cammen, L. A. (1991): Annual bacterial production in

relation to benthic microalgal production and sediment oxygen uptake in an intertidal sandflat and intertidal mudflat. *Mar. Ecol. Prog. Ser.* **71:**13–25.

Christensen, B., Vedel, A., and Kristensen, E. (2000a): Carbon and nitrogen fluxes in sediment inhabited by suspension-feeding (*Nereis diversicolor*) and non-suspension-feeding (*N. Virens*) polychaetes. *Mar. Ecol. Prog. Ser.* **192:**203–217.

Christensen, P. B., Rysgaard, S., Sloth, N. P., Dalsgaard, T., and Schwærter, S. (2000b): Sediment mineralization, nutrient fluxes, denitrification and dissimilatory nitrate reduction to ammonium in an estuarine fjord with sea cage trout farms. *Aquat. Microb. Ecol.* **21:** 73–84.

Colijn, F., and de Jonge, V. N. (1984): Primary production of microphytobenthos in the Ems-Dollard estuary. *Mar. Ecol. Prog. Ser.* **14:**185–196.

Cowan, J. L. W., Pennock, J. R., and Boynton, W. R. (1996): Seasonal and interannual patterns of sediment-water nutrient and oxygen fluxes in Mobile Bay, Alabama (USA): regulating factors and ecological significance. *Mar. Ecol. Prog. Ser.* **141:**229–245.

Davey, J. T., and Partridge, V. A. (1998): The macrofaunal communities of the Skeffling muds (Humber estuary), with special reference to bioturbation. In: Black, K. S., Paterson, D. M., and Cramp, A. (eds) Sedimentary processes in the intertidal zone. The Geological Society, London, p 115–124.

Deflaun, M. F., and Mayer, L. M. (1983): Relationships between bacteria and grain surfaces in intertidal sediments. *Limnol. Oceanogr.* **28:**873–881.

de Jonge, V. N., and van Beusekom, J. E. E. (1995): Wind- and tide-induced resuspension of sediment and microphytobenthos from tidal flats in the Ems estuary. *Limnol. Oceanogr.* **40:**766–778.

Deming, J. W., and Baross, J. A. (1993): The early diagenesis of organic matter: bacterial activity. In: Engel, M. H., and Macko, S. A. (eds) Organic geochemistry. Plenum Publishing Corp., New York, N.Y., p 119–144.

Dolphin, T. J., Hume, T. M., and Parnell, K. E. (1995): Oceanographic processes and sediment mixing on a sand flat in an enclosed sea, Manukau Harbor, New Zealand. *Mar. Geol.* **128:**169–181.

Drabsch, J. M., Parnell, K. E., Hume, T. M., and Dolphin, T. J. (1999): The capillary fringe and the water table in an intertidal estuarine sand flat. *Estuar. Coast. Shelf Sci.* **48:**215–222.

Dye, A. H. (1983): A method for the quantitative estimation of bacteria from mangrove sediments. *Estuar. Coast. Shelf Sci.* **17:**207–212.

Eco-Port Technical Working Group (1998): Manual on the harmonization of port structures and tidal flats. Waterfront Vitalization and Environment Research Center, Tokyo, p 1–39 (in Japanese).

Ellery, W. N., and Schleyer, M. H. (1984): Comparison of homogenization and ultrasonication as techniques in extracting attached sedimentary bacteria. *Mar. Ecol. Prog. Ser.* **15:**247–250.

Epstein, S. S., and Rossel, J. (1995): Enumeration of sandy sediment bacteria: search for optimal protocol. *Mar. Ecol. Prog. Ser.* **117:**289–298.

Epstein, S. S., Alexander, D., Cosman, K., Dompé, A., Gallagher, S., Jarsobski, J., Laning, E., Martinez, R., Panasik, G., Peluso, C., Runde, R., and Timmer, E. (1997): Enumeration of sandy sediment bacteria: are the counts quantitative or relative? *Mar. Ecol. Prog. Ser.* **151:**11–16.

Falcão, M., and Vale, C. (1990): Study of the Ria Formosa ecosystem: benthic nutrient remineralization and tidal variability of nutrients in the water. *Hydrobiol.* **207:**137–146.

Falcão M., and Vale, C. (1998): Sediment-water exchanges of ammonium and phosphate in intertidal and subtidal areas of a mesotidal coastal lagoon (Ria Formosa). *Hydrobiol.* **373/374:**193–201.

Fenchel, T. (1984): Suspended marine bacteria as a food source. In: Fasham, M. J. R. (ed) Flows of energy and materials in marine ecosystems. Plenum Publishing Corp., New York, N.Y., p 301–305.

Fenchel, T., King, G. M., and Blackburn, T. H. (1998): Bacterial biogeochemistry: the ecophysiology of mineral cycling. Academic Press, San Diego, California.

Gilbert, F. G., Souchu, P., Bianchi, M., and Bonin, P. (1997): Influence of shellfish farming activities on nitrification, nitrate reduction to ammonium and denitrification at the water-sediment interface of the Thau lagoon, France. *Mar. Ecol. Prog. Ser.* **151:**143–153.

Goulletquer, P., Heral, M., Deslous-Paoli, J. M., Prou, J., Garnier, J., Razet, D., and Boromthanarat, W. (1989): Ecophysiologie et bilan énergétique de la palourde japonaise d'élevage *Ruditapes philippinarum*. *J. Exp. Mar. Biol. Ecol.* **132:**85–108.

Harvey, J. W., and Odum, W. E. (1990): The influence of tidal marshes on upland groundwater discharge into estuaries. *Biogeochem.* **10:**217–236.

Hemond, H. F., and Fifield, J. L. (1982): Subsurface flow in salt marsh peat: a model and field study. *Limnol. Oceanogr.* **27:**126–136.

Henriksen, K., Hansen, J. I., and Blackburn, T. H. (1981): Rates of nitrification, distribution of nitrifying bacteria, and nitrate fluxes in different types of sediment from Danish waters. *Mar. Biol.* **61:**299–304.

Henriksen, K., and Kemp, W. M. (1988): Nitrification in estuarine and coastal marine sediments. In: Blackburn, T. H., and Sørensen, J. (eds) Nitrogen cycling in coastal marine environments. John Wiley & Sons, New York, N.Y., p 207–249.

Herbert, R. A., and Nedwell, D. B. (1990): Role of en-

vironmental factors in regulating nitrate respiration in intertidal sediments. In: Revsbech, N. P., and Sørensen, J. (eds) Denitrification in soil and sediment. Plenum Press, New York, N.Y., p 77–90.

Hillebrand, H., and Sommer, U. (1999): The nutrient stoichiometry of benthic microalgal growth: Redfield proportions are optimal. *Limnol. Oceanogr.* **44:**440–446.

Hosokawa, Y. (2000): Preservation and restoration of tidal flat ecosystem. In: Sudo, R. (ed) Ecological engineering for the restoration of ecosystems. Kodansya, Tokyo, p 191–224 (in Japanese).

Howes, B. L., and Goehringer, D. D. (1994): Porewater drainage and dissolved organic carbon and nutrient losses through the intertidal creekbanks of a New England salt marsh. *Mar. Ecol. Prog. Ser.* **114:**289–301.

Hughes, D. J., Atkinson, R. J. A., and Ansell, A. D. (2000): A field test of the effects of megafaunal burrows on benthic chamber measurements of sediment-water solute fluxes. *Mar. Ecol. Prog. Ser.* **195:**189–199.

Imai, I. (1987): Size distribution, number and biomass of bacteria in intertidal sediments and seawater of Ohmi Bay, Japan. *Bull. Jpn. Soc. Microb. Ecol.* **2:**1–11.

Inoue, T., and Nakamura, Y. (2000): Response of sediment oxygen demand and phosphate release rate to a staircase change in DO concentration and flow velocity. *J. Hydrosci. Hydraul. Eng.* **18:**183–193.

Jenkins, M. C., and Kemp, W. M. (1984): The coupling of nitrification and denitrification in two estuarine sediments. *Limnol. Oceanogr.* **29:**609–619.

Jørgensen, B. B., and Sørensen, J. (1985): Seasonal cycles of O_2, NO_3^- and SO_4^{2-} reduction in estuarine sediments: the significance of an NO_3^- reduction maximum in spring. *Mar. Ecol. Prog Ser.* **24:**65–74.

Joye, S. B., and Paerl, H. W. (1993): Contemporaneous nitrogen fixation and denitrification in intertidal microbial mats: rapid response to runoff events. *Mar. Ecol. Prog. Ser.* **94:**267–274.

Kaplan, W. A., Teal, J. M., and Valiela, I. (1977): Denitrification in saltmarsh sediments: evidence for seasonal temperature selection among populations of denitrifiers. *Microb. Ecol.* **3:**193–204.

Kasper, H. F., Gillespie, P. A., Boyer, I. C., and Mackenzie, A. L. (1985): Effects of mussel aquaculture on the nitrogen cycle and benthic communities in Kenepuru Sound, New Zealand. *Mar. Biol.* **85:**127–136.

Kemp, P. F. (1987): Potential impact on bacteria by grazing by a macrofaunal deposit-feeder, and the fate of bacterial production. *Mar. Ecol. Prog. Ser.* **36:** 151–161.

Kemp, W. M., Sampou, P. A., Garber, J., Tuttle, J., and Boynton, W. R. (1992): Seasonal depletion of oxygen from bottom waters of Chesapeake Bay: roles of benthic and planktonic respiration and physical exchange processes. *Mar. Ecol. Prog. Ser.* **85:**137–152.

Kerner, M., Kausch, H., and Miehlich, G. (1990): The effect of tidal action on the transformations of nitrogen in freshwater tidal flat sediments. *Arch. Hydrobiol.* **75:**251–271.

Kerner, M. (1993): Coupling of microbial fermentation and respiration processes in an intertidal mudflat of the Elbe estuary. *Limnol. Oceanogr.* **38:**314–330.

Kikuchi, E. (1986): Contribution of the polychaeta, *Neanthes japonica* (Izuka), to the oxygen uptake and carbon dioxide production of an intertidal mud-flat of the Nanakita River estuary. *J. Exp. Mar. Biol. Ecol.* **97:**81–93.

Koch, M. S., Maltby, E., Oliver, G.A., and Bakker, S. A. (1992): Factors controlling denitrification rates of tidal mudflats and fringing salt marshes in Southwest England. *Estuar. Coast. Shelf Sci.* **34:**471–485.

Kodama, M., Matsunaga, N., and Mizuta, K. (2000): Field observations of nutrient fluxes between tidal flat sediment and sea water. *Proc. Coast. Eng. Jpn. Soc. Civil Eng.* **47:**1126–1130 (in Japanese).

Koike, I., and Hattori, A. (1978): Simultaneous determinations of nitrification and nitrate reduction in coastal sediments by a ^{15}N dilution technique. *Appl. Environ. Microbiol.* **35:**853–857.

Koike, I., and Sørensen, J. (1988): Nitrate reduction and denitrification in marine sediments: microbial activities and fluxes. In: Blackburn, T. H., and Sørensen, J. (eds) Nitrogen cycling in coastal marine environments. John Wiley & Sons, New York, N.Y., p 251–273.

Kristensen, E. (1985): Oxygen and inorganic nitrogen exchange in a *Nereis virens* (Polychaeta) bioturbated sediment-water system. *J. Coast. Res.* **1:**109–116.

Kristensen, E. (1988): Benthic fauna and biogeochemical processes in marine activities and fluxes. In: Blackburn, T. H., and Sørensen, J. (Eds) Nitrogen cycling in coastal marine environments. John Wiley and Sons, New York, N.Y., p 275–299.

Kurihara, Y. (1988): Ecology and ecotechnology in estuarine-coastal area. Tokai University Publication, Tokyo (in Japanese).

Kuwae, T., Hosokawa, Y., and Eguchi, N. (1998): Dissolved inorganic nitrogen cycling in Banzu intertidal sand-flat, Japan. *Mangroves Salt Marshes* **2:**167–175.

Kuwae, T., and Hosokawa, Y. (1999): Determination of abundance and biovolume of bacteria in sediments by dual staining with 4′,6-diamidino-2-phenylindole and acridine orange: relationship to dispersion treatment and sediment characteristics. *Appl. Environ. Microbiol.* **65:**3407–3412.

Li, Y. H., and Gregory, S. (1974): Diffusion of ions in

sea water and deep-sea sediments. *Geochim. Cosmochim. Acta* **38:**703–714.

Lorenzen, C. J. (1967): Determination of chlorophyll and pheopigments: spectrophotometric equations. *Limnol. Oceanogr.* **12:**343–346.

Magni, P., Montani, S., Takada, C., and Tsutsumi, H. (2000): Temporal scaling and relevance of bivalve nutrient excretion on a tidal flat of the Seto Inland Sea, Japan. *Mar. Ecol. Prog. Ser.* **198:**139–155.

Malone, T. C., Garside, C., Haines, K. C., and Roels, O. A. (1975): Nitrate uptake and growth of *Chaetoceros* sp. in large outdoor continuous cultures. *Limnol. Oceanogr.* **20:**9–19.

Mann, R. (1979): The effect of temperature on growth and gametogenesis in the Manila clam *Tapes philippinarum* (Adams and Reeve, 1850). *J. Exp. Mar. Biol. Ecol.* **38:**121–133.

Maritime Safety Agency (1999): Tide tables volume 1 — Japan and its vicinities. Japan Hydrographic Association, Tokyo.

Mathieson, A. C., and Nienhuis, P. H. (1991): Intertidal and littoral ecosystems. Elsevier, New York, N.Y.

McLachlan, A., and Illenberger, W. (1986): Significance of groundwater nitrogen input to a beach/surf zone ecosystem. *Stygologia* **2:**291–296.

Mesnage, V., and Picot, B. (1995): The distribution of phosphate in sediments and its relation with eutrophication of a Mediterranean coastal lagoon. *Hydrobiol.* **297:**29–41.

Meyer-Reil, L. A. (1983): Benthic response to sedimentation events during autumn to spring at a shallow water station in the Western Kiel Bight. *Mar. Biol.* **77:**247–256.

Middelburg, J. J., Klaver, G., Nieuwenhuize, J., and Vlug, T. (1995): Carbon and nitrogen cycling in intertidal sediments near Doel, Scheldt Estuary. *Hydrobiol.* **311:**57–69.

Middelburg, J. J., Klaver, G., Nieuwenhuize, J., Wielemaker, A., de Haas, W., Vlug, T., and van der Nat, J. F. W. A. (1996): Organic matter mineralization in intertidal sediments along an estuarine gradient. *Mar. Ecol. Prog. Ser.* **132:**157–168.

Miller-Way, T., and Twilley, R. R. (1996): Theory and operation of continuous flow systems for the study of benthic-pelagic coupling. *Mar. Ecol. Prog. Ser.* **140:** 257–269.

Montagna, P. A. (1982): Sampling design and enumeration statistics for bacteria extracted from marine sediments. *Appl. Environ. Microbiol.* **43:**1366–1372.

Montagna, P. A. (1984): In situ measurement of meiobenthic grazing rates on sediment bacteria and edaphic diatoms. *Mar. Ecol. Prog. Ser.* **18:**119–130.

Montani, S., Magni, P., Shimamoto, M., Abe, N., and Okutani, K. (1998): The effect of a tidal cycle on the dynamics of nutrients in a tidal estuary in the Seto Inland Sea, Japan. *J. Oceanogr.* **54:**65–76.

Mortimer, R. J. G., Davey, J. T., Krom, M. D., Watson, P. G., Frinkers, P. E., and Clifton, R. J. (1999): The effect of macrofauna on porewater profiles and nutrient fluxes in the intertidal zone of the Humber estuary. *Estuar. Coast. Shelf Sci.* **48:**683–699.

Mukai, H. (1993): Comparison of Tokyo Bay with Seto Inland Sea. In: Ogura, N. (ed) Tokyo Bay — Environmental changes in the past century. Koseisha-Koseikaku, Tokyo, p 160 (in Japanese).

Nakanishi, H. (1993): Benthos. In: Ogura, N. (ed) Tokyo Bay — Environmental changes in the past century. Koseisha-Koseikaku, Tokyo, p 77–101 (in Japanese).

Nakata, K., and Hata, K. (1990): Evaluation of nutrient cycle in tidal flat. *J. Jpn. Soc. Water Environ.* **17:** 158–166 (in Japanese).

Nedwell, D. B., and Trimmer, M. (1996): Nitrogen fluxes through the upper estuary of the Great Ouse, England: the role of the bottom sediments. *Mar. Ecol. Prog. Ser.* **142:**273–286.

Nishio, T., Koike, I., and Hattori, A. (1982): Denitrification, nitrate reduction, and oxygen consumption in coastal and estuarine sediments. *Appl. Environ. Microbiol.* **43:**648–653.

Nuttle, W. K. (1988): The extent of lateral water movement in the sediments of a New England salt marsh. *Water Resour. Res.* **24:**2077–2085.

Ochi, T., and Takeoka, H. (1986): The anoxic water mass in Hiuchi-Nada part 1. Distribution of the anoxic water mass. *J. Oceanogr. Soc. Jpn.* **42:**1–11.

Odum, E. P. (1971): Fundamentals of ecology, 3rd ed. W. B. Saunders, Philadelphia.

Oglivie, B., Nedwell, D. B., Harrison, R. M., Robinson, A., and Sage, A. (1997): High nitrate, muddy estuarine as nitrogen sinks: the nitrogen budget of the River Colne estuary (United Kingdom). *Mar. Ecol. Prog. Ser.* **150:**21–228.

Ottosen, L. D. M., Risgaard-Petersen, N., Nielsen, L. P., and Dalsgaard, T. (2001): Denitrification in exposed intertidal mud-flats, measured with a new ^{15}N-ammonium spray technique. *Mar. Ecol. Prog. Ser.* **209:**35–42.

Parkin, T. B. (1990): Characterizing the variability of soil denitrification. In: Revsbech, N. P., and Sørensen, J. (eds) Denitrification in soil and sediment. Plenum Press, New York, N.Y. p 213–228.

Ports and Harbours Bureau, Ministry of Transport, Japan (1997): Eco-port — the port and harbour harmonized with natural environments —, Printing Bureau, Ministry of Finance, Japan, Tokyo (in Japanese).

Reay, W. G., Gallagher, D. L., and Simmons, G. M. Jr. (1995): Sediment-water column oxygen and nutrient fluxes in nearshore environments of the lower Delmarva Peninsula, USA. *Mar. Ecol. Prog. Ser.* **118:**

215–227.

Redfield, A. C., Ketchum, B. H., and Richards, F. A. (1963): The influence of organisms on the composition of sea-water. In: Hill, N. M. (ed) The sea, Vol 2. Wiley-Interscience, New York, N.Y., p 26–77.

Rizzo, W. M. (1990): Nutrient exchanges between the water column and a subtidal benthic microalgal community. *Estuaries* **13:**219–226.

Rizzo, W. M., Lackey, G. J., and Christian, R. R. (1992): Significance of euphotic, subtidal sediments to oxygen and nutrient cycling in a temperate estuary. *Mar. Ecol. Prog. Ser.* **86:**51–61.

Rocha, C., Cabeçadas, G., and Brogueira, M. J. (1995): On the importance of sediment-water exchange processes of ammonia to primary production in shallow areas of the Sado estuary (Portugal). *Neth. J. Aquat. Ecol.* **29:**265–273.

Rocha, C. (1998): Rhythmic ammonium regeneration and flushing in intertidal sediments of the Sado estuary. *Limnol. Oceanogr.* **43:**823–831.

Rocha, C., and Cabral, A. P. (1998): The influence of tidal action on porewater nitrate concentration and dynamics in intertidal sediments of the Sado estuary. *Estuaries* **21:**635–645.

Rosenberg, R., and Loo, L. O. (1988): Marine eutrophication induced oxygen deficiency: effects on soft bottom fauna, western Sweden. *Ophelia* **29:**213–225.

Rublee, P. A. (1982): Seasonal distribution of bacteria in salt marsh sediments in North Carolina. *Estuar. Coast. Shelf Sci.* **15:**67–74.

Rutgers van der Loeff, M. M., Anderson, L. G., Hall, J., Iverfeldt, Å., Josefson, A. B., Sundby, B., and Westerlund, S. F. G. (1984): The asphyxiation technique: An approach to distinguishing between molecular diffusion and biologically mediated transport at the sediment-water interface. *Limnol. Oceanogr.* **29:**675–686.

Rysgaard, S., Christensen, P. B., and Nielsen, L. P. (1995): Seasonal variation in nitrification and denitrification in estuarine sediment colonized by benthic microalgae and bioturbating infauna. *Mar. Ecol. Prog. Ser.* **126:**111–121.

Rysgaard, S., and Berg, P. (1996): Mineralization in a northeastern Greenland sediment: mathematical modelling, measured sediment pore water profiles and actual activities. *Aquat. Microb. Ecol.* **11:**297–305.

Sasaki, K. (1989): Material circulation in intertidal flat. Bull. Coast. Oceanogr. 26:172–190 (in Japanese).

Sayama, M. (2000): Case studies in Koajiro Bay and Tokyo Bay. In: Koike, I. (ed) Analyses of nitrogen cycling at the sediment-water interface. Japan Environmental Management Association for Industry, Tokyo, p 68–81 (in Japanese).

Sayama, M. (2001): Presence of nitrate-accumulating sulfur bacteria and their influence on nitrogen cycling in a shallow coastal marine sediment. *Appl. Environ. Microbiol.* **67:**3481–3487.

Schallenberg, M., Kalff, J., and Rasmussen, J. B. (1989): Solutions to problems in enumerating sediment bacteria by direct counts. *Appl. Environ. Microbiol.* **55:**1214–1219.

Schmidt, J. L., Deming, J. W., Jumars, P. A., and Keil, R. G. (1998): Constancy of bacterial abundance in surficial marine sediments. *Limnol. Oceanogr.* **43:** 976–982.

Seitzinger, S. P. (1988): Denitrification in freshwater and coastal marine ecosystems: ecological and geochemical significance. *Limnol. Oceanogr.* **33:**702–724.

Slomp, C. P., Malschaert, J. F. P., and Van Raaphorst, W. (1998): The role of adsorption in sediment-water exchange of phosphate in North Sea continental margin sediments. *Limnol. Oceanogr.* **43:**832–846.

Sundareshwar, P. V., and Morris, J. T. (1999): Phosphorus sorption characteristics of intertidal marsh sediments along an estuarine salinity gradient. *Limnol. Oceanogr.* **44:**1693–1701.

Sundbäck, K., Enoksson, V., Granneli, W., and Petersson, K. (1991): Influence of sublittoral microphytobenthos on the oxygen and nutrient flux between sediment and water: a laboratory continuous-flow study. *Mar. Ecol. Prog. Ser.* **74:**263–279.

Suzumura, M., Ueda, S., and Sumi, E. (2000): Control of phosphate concentration through adsorption and desorption processes in groundwater and seawater mixing at sandy beaches in Tokyo Bay, Japan. *J. Oceanogr.* **56:**667–673.

Sweerts, J. P. R. A., Kelly, C. A., Rudd, J. W. M., Hesslein, R., and Cappenberg, T. E. (1991): Similarity of whole-sediment molecular diffusion coefficients in freshwater sediments of low and high porosity. *Limnol. Oceanogr.* **36:**335–342.

Thornton, D. C. O., Underwood, G. J. C., and Nedwell, D. B. (1999): Effect of illumination and emersion period on the exchange of ammonium across the estuarine sediment-water interface. *Mar. Ecol. Prog. Ser.* **184:**11–20.

Trimmer, M., Nedwell, D. B., Sivyer, D. B., and Malcolm, S. J. (1998): Nitrogen fluxes through the lower estuary of the Great Ouse, England: the role of the bottom sediments. *Mar. Ecol. Prog. Ser.* **163:**109–124.

Trimmer, M., Nedwell, D. B., Sivyer, D. B., and Malcolm, S. J. (2000): Seasonal benthic organic matter mineralisation measured by oxygen uptake and denitrification along a transect of the inner and outer River Thames estuary, UK. *Mar. Ecol. Prog. Ser.* **197:**103–119.

Uchiyama, Y., Nadaoka, K., Rölke, P., Adachi, K., and Yagi, H. (2000): Submarine groundwater discharge into the sea and associated nutrient transport in a

sandy beach. *Water Resour. Res.* **36:**1467–1479.
Underwood, G. J. C., Paterson, D. M., and Parkers, R. J. (1995): The measurement of microbial carbohydrate exopolymers from intertidal sediments. *Limnol. Oceanogr.* **40:**1243–1253.
Usui, T., Koike, I., and Ogura, N. (1998): Tidal effect on dynamics of pore water nitrate in intertidal sediment of a eutrophic estuary. *J. Oceanogr.* **54:**205–216.
van Duyl, F. C., van Raaphorst, W., and Kop, A. J. (1993): Benthic bacterial production and nutrient sediment-water exchange in sandy North sea sediments. *Mar. Ecol. Prog. Ser.* **100:**85–95.
Varela, M., and Penas, E. (1985): Primary production of benthic microalgae in an intertidal sand flat of the Ria de Arosa, NW Spain. *Mar. Ecol. Prog. Ser.* **25:** 111–119.
Venji, M. I., and Albright, L. J. (1986): Microscopic enumeration of attached marine bacteria of seawater, marine sediment, fecal matter, and kelp blade samples following pyrophosphate and ultrasound treatments. *Can. J. Microbiol.* **32:**121–126.
Vidal, M., and Morguí, J. A. (1995): Short-term pore water ammonium variability coupled to benthic boundary layer dynamics in Alfacs Bay, Spain (Ebro Delta, NW Mediterranean). *Mar. Ecol. Prog. Ser.* **118:**229–236.
Webster, I. T. (1992): Wave enhancement of solute exchange within empty burrows. *Limnol. Oceanogr.* **37:**630–643.
Webster, I. T., Norquay, S. J., Ross, F. C., and Wooding, R. A. (1996): Solute exchange by convection within estuarine sediments. *Estuar. Coast. Shelf Sci.* **42:**171–183.
Weise, W., and Rheinheimer, G. (1978): Scanning electron microscopy and epifluorescence investigation of bacterial colonization of marine sand sediments. *Microb. Ecol.* **4:**175–188.
Williams, P. J. L., Raine, R. C. T., and Bryan, J. R. (1979): Agreement between the C-14 and oxygen methods of measuring phytoplankton production reassessment of the photosynthetic quotient. *Oceanol. Acta* **2:**411–416.
Yamamuro, M., and Koike, I. (1998): Concentrations of nitrogen in sandy sediments of a eutrophic estuarine lagoon. *Hydrobiol.* **386:**37–44.
Yelverton, G. F., and Hackney, C. T. (1986): Flux of dissolved organic carbon and pore water through the substrate of a *Spartina alterniflora* marsh in North Carolina. *Estuar. Coast. Shelf Sci.* **22:**255–267.

Abbreviations

ANOVA: analysis of variance
AO: acridine orange
ATU: allylthiourea
DAPI: 4′,6-diamidino-2-phenylindole
Eh: redox potential
EPS: extracellular polymeric substances
NH_4^+: ammonium
NO_2^-: nitrite
NO_3^-: nitrate
PAR: photosynthetically available (active) radiation
PO_4^{3-}: phosphate
SE: standard error
SNK test: Student-Newman-Keuls multiple-comparison test